



Steel characteristics and their link to chip breaking and tool wear in metal cutting

Niclas Ånmark

Doctoral Thesis in Materials Science and Engineering
Stockholm 2016

Akademisk avhandling som med tillstånd av Kungliga Tekniska Högskolan i Stockholm, framlägges för offentlig granskning för avläggande av teknologie doktorsexamen, onsdagen den 8 juni 2016, kl. 10.00 i hörsal B3, Brinellvägen 23, Kungliga Tekniska Högskolan, Stockholm

KTH Royal Institute of Technology
School of Industrial Engineering and Management
Department of Materials Science and Engineering
Division of Applied Process Metallurgy
SE-100 44 Stockholm, Sweden

ISBN 978-91-7595-949-8

Cover: Reprinted with permission of Sandvik Coromant

Copyright © Niclas Ånmark, 2016

This thesis is available in electronic version at kth.diva-portal.org

Printed by US-AB, Stockholm, Sweden

Abstract

The vision of this thesis is to study how it is possible to obtain optimised workpieces during metal cutting processes in industry. Specifically, the work is aimed to increase the understanding between the steel characteristics and their link to the chip breaking and tool wear during metal cutting. The emphasis is on the influence of the cleanliness and the characteristics of non-metallic inclusions in the workpiece on the machinability of carburising steel grades. The machinability of a case hardening steel is improved by a M-treatment (additions of Ca). Also, the improved machinability of the M-steels offers an attractive potential to save money which makes it possible to reduce the tooling costs with up to 50%. The improved machinability of Ca-treated steels is correlated to the formation of lubricating slag layers consisting of Ca-enriched sulfide inclusions and oxy-sulfide inclusions, which are formed on the rake face during the machining operation. It is proposed that the formations of slag layers from the workpiece constituents are essential to minimise the chemical degradation of the tool edge due to a contact with the chip. During this process, sulfur minimises the material transfer from the chip flow, whilst Ca-treated impurities have a stabilising effect on the protective deposits made of slag layers.

Since there is a remaining industrial need to increase the production rate, whilst maintaining a high quality of the finished parts, the future production will continue to require extreme demands on the quality of workpieces. If the emphasis is focused on the workpiece, it should be possible to obtain a robust manufacturing process. Therefore, the challenge for future steel metallurgists is to develop high performance grades with optimised *combined* properties.

Keywords: machinability, steel, non-metallic inclusions.

Sammanfattning

Syftet med denna avhandling är att studera hur det är möjligt att framställa optimala ämnen för skärande bearbetning i industriell skala. Målsättningen med arbetet är att öka förståelsen för ståls egenskaper och dess inverkan på spånbrytning och slitage av verktyg vid skärande bearbetning. Avhandlingen fokuserar på kopplingen mellan arbetsstyckets renhet och inneslutningskaraktäristik och dess inverkan på skärbarhet hos sätthärtningsstål. Skärbarheten hos vanligt sätthärtningsstål kan förbättras markant genom en Ca-behandling, dvs. en så kallad M-behandling. Den förbättrade skärbarheten hos M-stål möjliggör stora kostnadsbesparingar, som uppskattas kunna reducera verktygskostnader med upp till 50%. Den förbättrade skärbarheten hos M-stål beror på bildningen utav tribologiska skikt som är anrikade med (Mn,Ca)S- och $(CaO)_x-Al_2O_3-S$ -slag. Dessa tribologiska skikt bildas på skärverktygets spånsida under ingrepp vid skärande bearbetning och består utav vissa atomer som överförs från det bearbetade ämnet till skäret. Bildandet av ett skyddande skikt anses nödvändigt för att undvika att verktygets skärepp utsätts för ett kemiskt angrepp i kontaktytan med spånflödet. Svavel anses minimera att rent arbetsmaterial överförs till skärverktyget medans kalcium-berikade inneslutningar hjälper till att bilda ett stabilt och skyddande tribologiskt skikt.

Det eviga behovet att öka produktionstakten, utan att för dess skull riskera slutproduktens kvalitet ställer stora krav på framtidens material. Med utgångspunkt från arbetsstycken så ska det vara möjligt att uppnå en robust industriell produktion. Utmaningen är därför att utveckla högpresterande stål med en förhöjd *kombinerad* funktionsegenskap.

Nyckelord: skärbarhet, stål, icke-metalliska inneslutningar.

Preface

This thesis summarises the knowledge I gained during my period as a Ph.D. candidate within the research area of applied process metallurgy. The work during the first two years was carried out partly at the Department of Materials Science and Engineering at KTH Royal Institute of Technology, Stockholm, Sweden and partly at the Department of Materials and Manufacturing at Swerea KIMAB whilst the final part was conducted at the Department of Advanced Engineering Transmission Production at Scania CV, Södertälje, Sweden. The work has been part of projects which was focused on the influence of non-metallic inclusions and microstructure on the machinability of carburising steel grades for soft and hard machining. The first project was conducted within the Member Research Consortium Materials in Machining at Swerea KIMAB. The second part was conducted within a VINNOVA funded project within the national Strategic Innovation Program - National Action for Metallic Materials. Participating companies were Sandvik Materials Technology, Sandvik Coromant, Ovako Hofors, Outokumpu Stainless, Uddeholm Tooling and Seco Tools. The final study was part of a process development project at Scania CV.

I thank the Axel Hultgren, the Gustav Jansson, the Gerhard Von Hofsten and the Hugo Carlsson foundations for their financial support.

This thesis will in particular discuss the following challenges:

- Some metallurgical aspects of modification and control of non-metallic inclusions to improve the machinability of steel.
- The effect of inclusion composition, size, morphology, and number on the tool wear mechanisms during machining of carburised steel. Non-metallic inclusions were characterised after observations in both 2D and 3D.

- The effect of grain size and micro hardness on the tool wear during soft machining of clean steel.
- The possibilities to differentiate the machinability of similar carburising steel grades by using different methods.
- The characteristics of different non-metallic inclusions in high performance steels to improve the *combined* performance of mechanical strength and machinability.

In this thesis, six papers are appended, as listed below. They will be referred to as Paper I-VI throughout the text. One conference proceeding is included in this thesis since it adds important results and discussions to the overall work. Another conference proceeding, describing important findings is also listed, but not included in this thesis. Also, as a milestone a licentiate thesis was written to summarise some of the initial findings of my graduate studies.

I hope that this thesis will give the reader a better understanding about non-metallic inclusions and their characteristics which needs to be considered in order to control the mechanical strength and machinability of high performance steel grades.

Niclas Ånmark
Stockholm, June 2016

List of papers

- I. The effect of different non-metallic inclusions on the machinability of steels
N. Ånmark, A. Karasev, P.G. Jönsson
Materials 8-2 (2015) 751-783
- II. The effect of cleanliness and micro hardness on the machinability of carburizing steel grades suitable for automotive applications
N. Ånmark, S. Lövquist, M. Vosough, T. Björk
Steel Research International 87 (2016) 403-412
- III. The influence of microstructure and non-metallic inclusions on the machinability of clean steels
N. Ånmark, A. Karasev, P.G. Jönsson
Submitted manuscript
- IV. The effect of inclusion composition on tool wear in hard part turning using PCBN cutting tools
N. Ånmark, T. Björk, A. Ganea, P. Ölund, S. Hogmark, A. Karasev, P.G. Jönsson
Wear 334-335 (2015) 13-22
- V. Effect of different inclusions on mechanical properties and machinability of 20NiCrMo carburizing steels
N. Ånmark, T. Björk, A. Karasev, P.G. Jönsson
Proceeding of the 6th International Congress on the Science and Technology of Steelmaking. Beijing: The Chinese Society for Metals, May 12-14th (2015) 805-808
- VI. Steel characteristics and their link to tool wear in hard part turning of transmission components
N. Ånmark, T. Björk
Submitted manuscript

The author's contribution to the papers:

- I. Parts of literature review and writing
- II. Parts of experimental work, major part of literature review, analysis and writing
- III. Major part of literature review, experimental work, analysis and writing
- IV. Major part of literature review, experimental work, analysis and writing
- V. Major part of literature review, experimental work, analysis and writing
- VI. Major part of literature review, experimental work, analysis and writing

Other relevant publications not included in the thesis:

- I. Inclusion characteristics and their link to tool wear in metal cutting of clean steels suitable for automotive applications
N. Ånmark
Licentiate thesis, KTH Royal Institute of Technology, Stockholm, Sweden, 2015
- II. Tool wear in soft part turning of high performance steel
N. Ånmark, T. Björk
Proceeding of the 7th CIRP Conference on High Performance Cutting. Chemnitz, May 31th – June 2nd (2016)

List of abbreviations

V_B	Flank wear. One cutting tool wear measure that is used to decide a cutting tool's service life time.
K_T	Crater depth. The other frequently used tool wear measure. Together they indicate the balance of the active wear mechanisms.
R_a	A measure that describes the roughness of a surface. It is the average deviation from the center line of a scanned surface. R_a was used in this thesis to characterise the machined surfaces.
WC	Tungsten carbide. Cutting tools that are made for soft machining of steel are primarily composed of WC grains that are glued together by a metallic binder.
PCBN	Polycrystalline cubic boron nitride. Cutting tools that are made for hard part turning are primarily composed of CBN grains that are glued together by a ceramic binder.
NMI	Non-metallic inclusions.
d_{eq}	Equivalent circular diameter. A parameter that is used to describe the size of non-metallic inclusions.
N_A	Number of non-metallic inclusions per unit area.
D_G	Grain size. A parameter that is used to describe the microstructure of a steel grade.
CE	Carbon equivalent. A concept that converts the content of alloying elements other than carbon to their equivalent carbon percentage.

HV	Hardness Vickers. A method that uses a pyramid-shaped indenter to approximate the hardness of steel. The method was used in this thesis to quantify the surface hardness and the profile of carburised steel.
LOM	Light optical microscopy. A method that was used to observe the cutting tool wear and the steel microstructure.
CLM	Confocal laser microscopy. A microscopy technique that allows a large depth of field. Thus, CLM was used to quantify the depth of the PCBN rake face crater wear.
SEM	Scanning electron microscopy. A microscopy technique that allows imaging at a higher resolution than LOM.
SE	Secondary electrons. Was detected and used to image the tool wear of used cutting tools.
BSE	Backscattered electrons. Was detected and used to image the tool wear of used cutting tools.
EDS	Energy dispersive spectroscopy. A feature of the SEM that allows for chemical analysis. EDS was used to analyse the tested steels and the used cutting tools.
EBSD	Electron backscatter diffraction. A feature of the SEM that allows for a crystallographic characterisation of any crystalline material. In this thesis, SEM-EBSD was used to estimate the average grain size of carbon steel.
EE	Electrolytic extraction. An extraction technique that together with the SEM allows for a three dimensional characterisation of non-metallic inclusions.

Contents

INTRODUCTION.....	1
1.1. RESEARCH OBJECTIVES	2
BACKGROUND.....	5
2.1. CLEAN STEEL	5
2.2. NON-METALLIC INCLUSIONS	6
2.3. CARBURISING STEEL PROCESSING	7
2.4. HEAT TREATMENT	8
2.5 METAL CUTTING.....	11
2.6. MACHINABILITY	12
2.7. CUTTING TOOLS.....	14
2.8. TOOL WEAR.....	15
EXPERIMENTAL.....	17
3.1. WORKPIECES	17
3.2. CUTTING TOOLS.....	19
3.3. MACHINABILITY STUDIES.....	20
3.4. CHARACTERISATION.....	23
RESULTS AND DISCUSSION.....	31
4.1. INCLUSION MODIFICATION AND CONTROL	31
4.2. NON-METALLIC INCLUSIONS IN CARBURISING STEELS	33
4.3. MICROSTRUCTURAL FEATURES OF CARBURISING STEEL	38
4.4. THE MACHINABILITY OF CARBURISING STEELS IN SOFT CONDITION.....	39
4.5. THE MACHINABILITY OF CARBURISING STEELS IN HARD CONDITION	43
4.6. MATERIAL TRANSFER DURING HARD PART TURNING	46
4.7. THE ROLE OF NON-METALLIC INCLUSIONS	50
4.8. COMPARISON BETWEEN STANDARD STEELS AND CLEAN STEELS	51
4.9. THE BUSINESS CASE OF THE M-STEEL	52
CONCLUDING DISCUSSION.....	53
CONCLUSIONS	57

FUTURE WORK.....	61
ACKNOWLEDGEMENTS.....	63
BIBLIOGRAPHY	65

CHAPTER 1

INTRODUCTION

Developments in steel production since the 1970's have resulted in steel grades with a reduced content of impurities. More specifically, so called "high cleanliness" steels have been introduced by the steelmakers around the world¹⁻⁸. Thereby, responding to the current and future market demands of steel having excellent fatigue strength and impact toughness and/or an improved corrosion resistance. Clean steels are associated with extremely low levels of impurities such as oxygen (< 10 ppm O) and sulfur (< 10 ppm S). The driving force behind these developments has been to provide new steels that can perform well in extremely challenging applications e.g., gearbox components for heavy trucks, bars for demanding construction and tubes for highly corrosive atmospheres.

Although the new clean and ultra-clean steels have an improved mechanical strength and/or an exceptional corrosion resistance, these advantages have come at the expense of a more difficult chip breaking and in a reduced cutting tool life^{9,10}. From an industrial point of view, metal cutting processing should always remove a certain volume of metal as fast as possible, to as low cost as possible, and still generate a product that meets the demands from the customer. The remaining issue is therefore to manufacture high performance steels with improved *combined* properties of mechanical strength and machinability.

1.1. Research objectives

The vision of this thesis is to allow optimised workpieces at metal cutting processes during an industrial production. With emphasis on the workpiece, it should be possible to have a robust manufacturing process.

This thesis is based on six papers (Fig. 1.1) and it aims to increase the understanding between steel characteristics and their link to chip breaking and tool wear in metal cutting. Within that scope, a literature review (Paper I) was conducted to summarise the effect of different non-metallic inclusions (NMI) and their characteristics on the machinability of various steels. Therefore, a comparison between different machining tests and their ability to differentiate the machinability between similar steel grades was conducted (Paper II). Moreover, the correlation between steel and inclusion composition on the tool life and tool wear mechanisms were evaluated during both soft and hard part turning (Paper III-V) on a lab scale. Also, some features of microstructure and mechanical properties were covered. Finally, a focused field study on the effect of the steel composition on the hard machining of gearbox products was conducted to verify that the findings in Paper IV,V can be transferred to an industrial production (Paper VI).

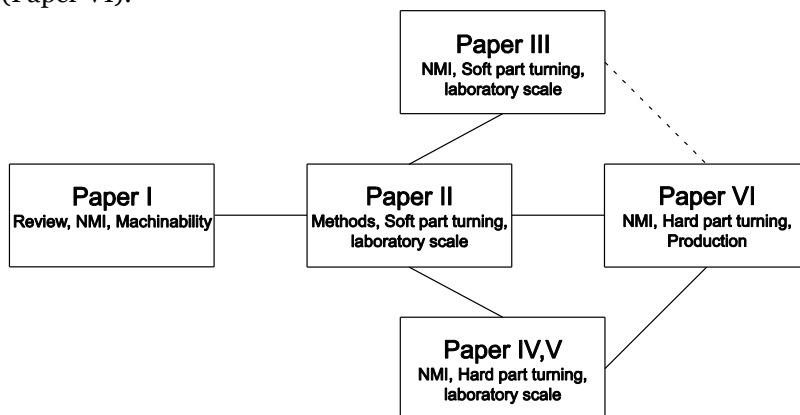


Fig. 1.1 Overview of the structure and the link between the appended papers.

An overview of the supplements and their objectives are summarised in Table 1.1.

Table 1.1 Overview of the main topics that are discussed in the thesis.

Paper	Study	Objective	Approach	Parameters
I	The effect of different NMI on the machinability of steels	Overview the characteristics of NMI and their link to machinability	Literature review of previous work	Steel and inclusion composition, d_{eq} , N_A , N_V , f_V , AR , V_B , K_T
II	The effect of steel cleanliness on the machinability of carburizing steel	Methods that can differentiate the machinability of similar steels	Soft part turning of a standard, a clean and an ultra-clean steel	Tool life, tool wear, chip formation, steel composition
III	The influence of microstructure and NMI on the machinability of clean steels	Correlations between microstructure and content of NMI to the cutting tool life	Soft part turning of a standard, a clean and an ultra-clean steel	CE , D_G , $HV_{0.5R}$, f_V , AR , tool life
IV	The effect of inclusion composition on tool wear	Link inclusion characteristics to PCBN cutting tool wear and tool life	Hard part turning of a standard, a Ca-treated, and two clean steels	Steel and inclusion composition, d_{eq} , N_A , V_B , K_T
V	Effect of different inclusions on machinability of 20NiCrMo steels	Link inclusion characteristics to PCBN cutting tool wear and tool life	Hard part turning of a standard, a Ca-treated and a clean steel	Steel and inclusion composition, d_{eq} , N_A , V_B , K_T
VI	Steel characteristics and their link to tool wear in hard part turning	Link steel composition to the PCBN cutting tool life at industrial production	Hard part turning of a standard and a Ca-treated steel grade at gearbox production	Steel and inclusion composition, tool life, V_B , K_T , R_a

Introduction

CHAPTER 2

BACKGROUND

2.1. Clean steel

The level of a steels' cleanliness can be defined by its content of harmful elements i.e. oxygen, sulfur, nitrogen and carbon, phosphorus and hydrogen¹¹. Steel cleanliness can also be defined by a low content of non-metallic inclusions where foremost oxides, sulfides, nitrides and carbides are considered^{9,11}. Since 1970, the level of impurities in steel has decreased from about 100 ppm to less than 10 ppm (Fig. 2.1)^{11,12}.

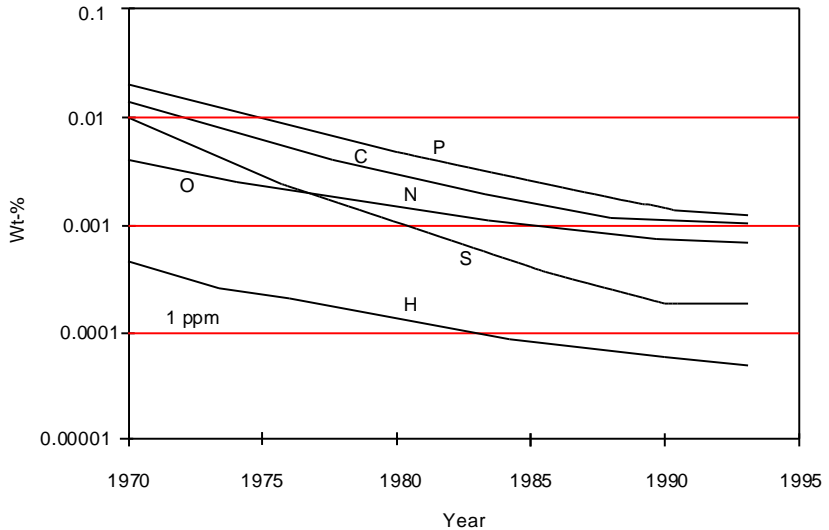


Fig. 2.1 Advances in steelmaking technology has enabled cleaner steel over time¹¹.

Background

The technology of clean steel is strongly linked to the concept of inclusion engineering and inclusion control¹³⁻¹⁵. From the view point of a steel manufacturer this implies that alloying and modifications of the liquid steel must be performed with regards to the inclusion characteristics. This is of particular importance at the later refining stages, i.e. during ladle and tundish treatment of liquid steels. At that point, there is a limited amount of time to modify the liquid melt before casting. Thus, it is a challenging task to remove additional inclusions that are added into the steel.

The fatigue strength and impact toughness of steel are strongly related to the maximum size and the size distribution of non-metallic inclusions¹⁶⁻¹⁸. Therefore, the size distribution of non-metallic inclusions can be used to predict a steels' mechanical performance. In turn, this method provides a faster analysis and makes it possible to avoid costly material characterisation of a large volume of steel. Therefore, it is of utmost importance to investigate the inclusion characteristics of steel.

2.2. Non-metallic inclusions

Non-metallic inclusions can have various physical properties and different influences on the machinability of steel. The five main characteristics that are used to describe non-metallic inclusions are composition, size, number, morphology and distribution. Today, there are many techniques available in the steelmaking industry for a correction and control of the characteristics of non-metallic inclusions. Based on an overview of present publications¹⁹, it can be concluded that to improve the machinability, there are four common techniques: (1) Increasing the sulfur content in the molten metal for a larger volume fraction of sulfide inclusions, (2) Modifying the existing sulfide inclusions (MnS) by a Ca-treatment of the molten steel or by additions of other strong sulfide formers such as Ca, REM or Zr, (3) Applying a Ca-treatment in order to modify the existing oxides in the molten metal (Al_2O_3 , Al_2O_3 -MgO, SiO_2) and (4) Adding rare elements

(Se, Te, B) to alter the properties of both the MnS and Al₂O₃ inclusions. The purpose of sulfur additions is to increase the amount of impurities that act as stress-raisers in the primary shear zone at the tool edge-chip interface during machining. A Ca-treatment aims primarily to alter the inclusion composition and shape with the objective to form globular and glassy complexes, which typically are composed of (Al,Mg)O-(Mn,Ca)S, which are softer than pure oxides. Thus, they are believed to be less detrimental for the cutting tool wear.

Characterisation of non-metallic inclusions are usually done in 2D by using SEM analyses on a cut-out cross-section from a steel piece²⁰. This technique is limited by the fact that the precise composition and shape of the evaluated inclusions cannot be determined. Furthermore, developments of newer techniques to treat samples such as electrolytic extraction allows for SEM observation of non-metallic inclusions in 3D²¹. Characterisation of impurities in 3D are believed to be more accurate, especially when it comes to the size, composition and the morphology of inclusions. One of the main advantages of electrolytic extraction is that very fine inclusions of sizes as small as 0.05 µm can be observed, which is not possible in 2D characterisation or by using chemical extraction with methanol alcohol or acids (HCl, HNO₃, H₂SO₄)^{22,23}.

2.3. Carburising steel processing

Conventional billet manufacturing includes a wide variety of processes, ranging from melting scrap to billet grinding (Fig. 2.2). Internal or domestic scrap are sorted and melted in an electric arc furnace (EAF). Thereafter, the liquid melt is tapped into a ladle or a converter vessel for refinement by additions of ferroalloys e.g. FeSi and FeAl. A ferroalloy serves as a deoxidiser of the molten steel and reduces its oxygen activity²⁴⁻²⁶. Thereafter, the slag that was formed during deoxidation is skimmed off. As the vessel enters the ladle furnace station, a synthetic top slag based on CaO and Al₂O₃ is added onto the liquid steel²⁷. The top slag serves as a protection against

Background

reoxidation whilst it simultaneously promotes a removal of non-metallic inclusions. Thereafter, the steel melt is deoxidised and desulfurised before the ladle is transported to a vacuum degassing station. At the degassing station, hydrogen and nitrogen is reduced by a combined argon gas and induction process, which is an effective approach to manufacture clean steels. Processes that occur in parallel are an adjustment of alloying composition, gas and magnetic stirring and reheating to reach the desired temperature before the melt is teemed into ingot moulds. In a mould, the melt is solidified as it is subjected to cooling. The workpiece is then stripped out of the mould and put in a pit furnace for a further temperature decrease. Then, the workpiece is plastically deformed by a number of hot-rolling processes into a billet with desired dimensions. Parallel processes include removal of oxide scale (scarfing) and quality inspection. A final grinding of the billet is then performed before it is delivered to the customer.

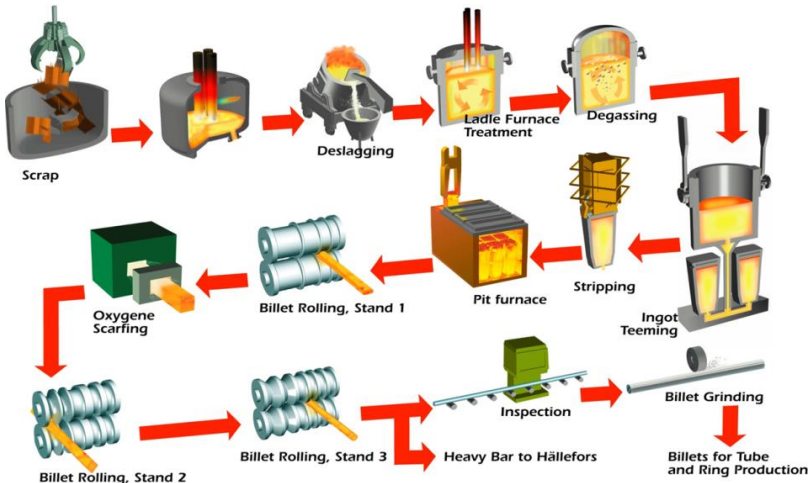


Fig. 2.2 A schematic illustration of the steel billet manufacturing at Ovako Hofors AB⁹.

2.4. Heat treatment

Heat treatment of steels is a critical process, because it strongly influences the final material properties. Case hardening steels are

usually annealed prior to soft machining to make the workpiece easy-to-cut and to form it into its desired shape. After soft machining, steels for automotive applications are usually carburised in order to obtain a hardened surface layer. Still, the core material is tough and of a more ductile character. Typically, the carburised layer has a hardness of 60 ± 2 HRC and a 1 mm thickness. The high surface hardness of carburised steel offers an attractive ability to withstand contact fatigue, which makes the material suitable for load-bearing applications such as transmission products. The carburising operation is a heat treatment that takes place in a furnace at an elevated temperature of about $850\text{--}950^\circ\text{C}$ under an atmospheric pressure rich in carbon monoxide (CO), nitrogen (N_2) and hydrogen (H_2). Subsequent processes to carburising are quenching and tempering (Fig. 2.3). The steel component hardens during quenching as the austenite part in the carburised layer is transformed into martensite.

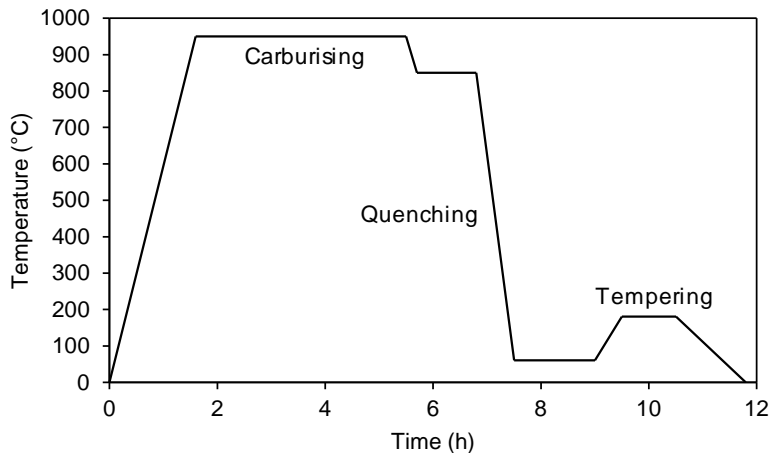


Fig. 2.3 A typical heat treatment cycle for a carburising operation of a case hardening steel²⁸.

Steels with a content of 0.1-0.3 wt-% carbon are typically carburised²⁸. The component is made up of a hard surface, which is beneficial for the fatigue strength. The core is somewhat softer, yet with a

Background

significantly increased toughness that is required to withstand mechanical shocks.

Hardenability improving elements are mainly Ni, Mn, Cr and Mo and they allow a higher phase transformation rate of austenite to martensite during quenching²⁹. The carbon content at the surface can vary between 0.65-1.1 wt-% C depending on the steel grade. However, steel grades with higher contents of carbon do not necessarily result in a higher surface hardness as their content of retained austenite is higher than in a low carbon steel grade. The maximum surface carbon content is often limited by the carbide formation that occurs at the given process temperatures.

Case hardening steel grades are frequently used for an industrial production, since they are easy to machine and have a high mechanical strength. In general, carburising steel grades can be classified into three major categories:

- 1) Conventional carburising steel grades typically used in transmission components, which contain 300-500 ppm sulfur¹². The sulfur level is balanced by the risk for inclusion induced fatigue and machinability.
- 2) Clean steels of a superior mechanical strength, by the minimum content of impurities^{11,12}, which may be as low as 20 ppm.
- 3) Machinability improved steel grades. Historically, such steel grades were made by additions of lead (Pb) or sulfur (600-1000 ppm)^{30,31}. These steels are often referred to as free-cutting steels. Nowadays, the improved machinability of structural steels is obtained by calcium deoxidation of molten steel to contents of 15-40 ppm Ca. However, for the Ca-treatment to be successful, it requires a sulfur content of about 200-400 ppm, in order to form oxy-sulfide impurities. A calcium deoxidation turns alumina into Ca-aluminates^{11,12}, which has a lower melting temperature than the pure oxides.

Thus, Ca-aluminates are associated with a lower risk for an abrasion of the cutting tool during machining^{32,33}, which can increase the cutting tool life. Simultaneously, (Mn,Ca)S inclusions are formed due to the Ca-treatment and they have a higher hardness than the pure MnS inclusions^{32,34}.

2.5 Metal cutting

Metal cutting refers to the numerous manufacturing processes which are used to produce components for e.g. the automotive and the construction industries. Depending on the specific application of the component to be machined, a wide range of metals, alloys and composites having different material characteristics, can be selected. Many machining processes exist today, but the most frequent in traditional production may be the turning and the milling operations. Other common machining processes include drilling, broaching and shaping. The mutual factor is that an insert is used for a metal removal in order to shape the workpiece and to produce a specified surface.

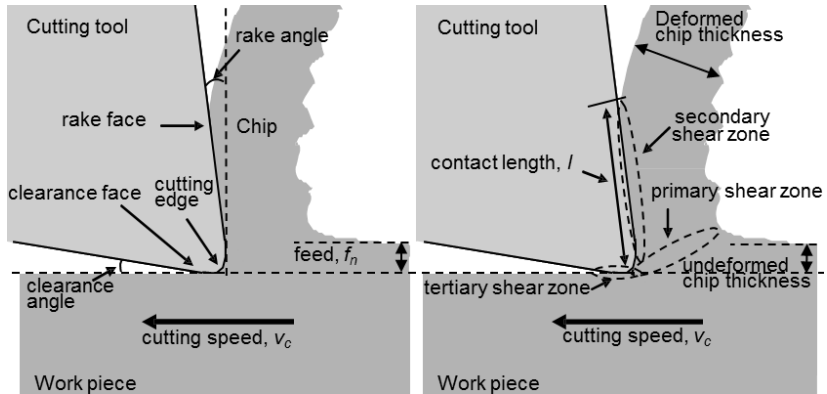


Fig. 2.4 Schematic illustrations of the chip formation process and the three shear zones in metal cutting³⁵.

The chip formation can be considered the main concept to describe the interaction between a cutting tool and a workpiece in metal cutting (Fig. 2.4). During a chip formation the workpiece rotates with a certain

Background

rate which is called the cutting speed (v_c , m/min). At the same time, the cutting edge travels a specified distance through the part according to its feed rate (f_n , mm/rev). Thus, this produces a chip. It results in the formation of two new surfaces of the cutting tool, the clearance and the rake face. The clearance face is linked to the generated surface roughness of the machined part. Therefore, it is necessary to use a clearance angle between the tool and the workpiece to avoid friction against the new surface. The rake face is the surface which is in contact with the chip flow, and the angle between the primary cutting edge and the normal to the surface being cut is called the rake angle¹². Depending on the material to machine, and the load to carry, the geometry of the cutting tool can vary in a wide range.

Machining is associated with a tremendous power consumption. It can be explained by the severe plastic deformation that occurs in the primary shear zone³⁶. In addition, a lot of energy is consumed as the deformed chip travels along the primary cutting edge, which results in a secondary shear zone. Finally, the tertiary deformation zone is the interaction zone between the machined part and the clearance face of the cutting tool. Hence, it is believed to be essential for the generated surface roughness.

2.6. Machinability

Machinability is a complex concept, which has several definitions. For example, it can be defined as follows:

“how readily a particular workpiece material can be machined by a cutting tool in a manner such that certain predetermined levels of form, size and degree of roughness of the surface can be achieved”³⁷

The complexity is caused by the fact that each machining practitioner interprets the machinability based on his individual experience. From a broader perspective, a machinability measure should indicate a materials' overall machinability and not merely for a certain product

or process. Therefore, the machinability concept can be divided into five sub-groups, i.e., a chip formation, a cutting tool wear, a cutting force, a power consumption, a surface integrity of the machined part, and an impact on the environment, as shown in Fig. 2.5.

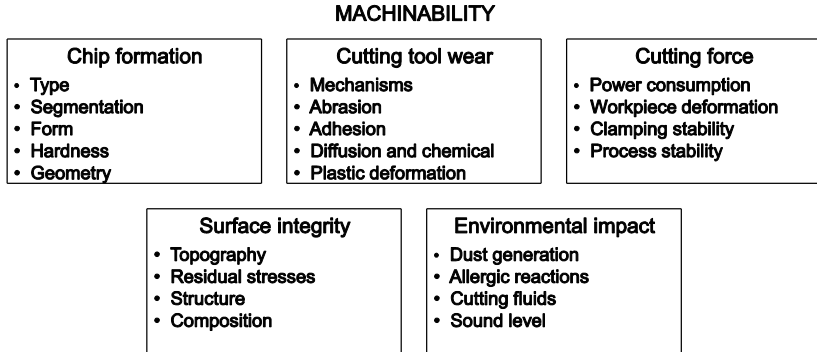


Fig. 2.5 The traditional view on the machinability concept including its sub-groups¹⁴.

The cutting tool life is one of the most common machinability indexes, because it is closely related to production economy. Therefore, it has been selected as the criterion in most of the papers in this thesis. Furthermore, machining processes are strongly related to the manufacturing costs. Specifically, Tönshoff and Stanske found that more than 40% of the total manufacturing cost to produce an automotive component comes from machining operations³⁸. Hence, an improved machinability can significantly reduce the total manufacturing cost.

In all machining operations, non-metallic inclusions can play an important role as they have the ability to ease a chip formation. A detailed explanation was published by Kiessling³⁹, who stated that metal cutting can be significantly improved when the inclusions:

- 1) Act as stress-raisers in the shear plane, which cause a crack formation. This, in turn, leads to embrittled chips that are easily broken. In addition, the length of the contact zone (l , see Fig. 2.4) between the chip and the cutting tool is reduced.

Background

Thus is advantageous for the tool wear resistance.

- 2) Are active in the metal flow zone, and contributes to shearing of the metal. However, an appropriate balance of inclusions is necessary to avoid an increased tool wear rate.
- 3) Form a diffusion barrier, isolating the rake face from diffusion-induced chemical tool wear at high temperatures.
- 4) Act as lubricant which protects the flank face of a cutting tool from an abrasive wear.

2.7. Cutting tools

Advances in cutting tool manufacturing since the beginning of the 19th century has led to new grades and new coating technologies, which offers a higher wear resistance, a higher toughness and a higher hot-hardness. Carbon steels were introduced around 1900, followed by high-speed steels (HSS) that were developed before the 1920's. Tungsten carbide (WC) was introduced in the 1930's, ceramics in the middle of the 1950's, followed by synthetic diamond in the late 1950's and coated carbide in the 1970's⁴⁰. Research developments during the last decades have resulted in ceramic cutting tools based on poly-crystalline cubic boron nitride (PCBN). This has provided new possibilities to further increase the industrial productivity and to improve the quality of the machined part as well as to reduce the cost. PCBN has been successfully introduced in hard part turning operations. Among others, it offers versatility less machine time and a partially elimination of coolant in the machining process, as compared to grinding.

The majority of the tools used for industrial machining of carbon steel are cemented carbides (soft machining) and PCBN (hard machining). They are therefore given an extra attention in this study.

A cemented carbide cutting tool is a composite of carbide grains which are glued together in a matrix of a metallic binder, often consisting of cobalt or nickel. The volume fraction of the carbide phase ranges from

0.6 to 0.95. Hence, the volume fraction of metallic binder ranges from 0.05 to 0.4. Overall, WC mixed with cobalt (Co) may be the most common substrate material. Other carbides are made of chromium (Cr), niobium (Nb), titanium (Ti) and tantalum (Ta). Cemented carbides are characterised by hardness levels higher than those of steel even though the hardness decrease with increasing temperature. The hardness and the toughness of the cemented carbide are highly dependent on composition and grain size. Therefore, they can be adjusted depending on application. Cemented carbides can be used to machine a wide range of workpieces, from carbon and stainless steel to grey cast iron. In addition, cemented carbides have a good thermal and electrical conductivity yet a low ability to withstand deformation without fracture. A good thermal conductivity correlates to the ability to dissipate heat away from the cutting zone. If necessary, it is possible to modify the surface properties of a cutting tool by deposition of ceramic coatings. Here, chemical vapour deposition (CVD) is used on the vast majority of cutting tools for turning. Examples of coatings are Al_2O_3 , AlCrN , TiN , TiC , TiCN , TiAlN , and ZrN . These ceramic coatings can serve to protect the cutting tool from a rapid tool degradation.

PCBN cutting tools are composed of about 50 to 90 vol% cubic boron nitride (CBN), which depends on the machining application⁴¹. The other part is made of a metallic binder such as cobalt or nickel, or by a ceramic binder, for instance titanium nitride^{42,43}. A reduced CBN content of the PCBN prolongs the cutting tool life⁴³ and promotes a finer surface roughness in metal cutting. Furthermore, the advantage of PCBN compared to cemented carbides is its ability to maintain its properties at elevated temperatures. The maintained hot-hardness, toughness and resistance to thermal shock^{44,45} explains why PCBN is suitable for hard part machining.

2.8. Tool wear

Wear mechanisms are in general of abrasive⁴⁵⁻⁵¹, adhesive⁴⁹⁻⁵¹ or chemical^{43,45,50-52} nature. Abrasion is caused by hard particles from the

Background

workpiece material that wears the cutting tool in a micro-ploughing manner. An adhesive wear can be described as a micro-welding process where small parts of the cutting tool are ripped off by the passing chip. A chemical wear is induced by a reaction in which atoms in the cutting tool are dissolved or diffused into the workpiece material. In addition, heavy plastic deformation may cause delamination of the cutting tool, which often leads to crack formation and edge failure.

Common wear patterns of a used cutting tool are a crater, a flank and a notch wear (Fig. 2.6). Flank wear is foremost linked to a continuous and abrasive wear acting on the flank face, whilst a crater wear appears on the rake face at very high temperatures in combination with a chemical attack and/or an abrasion. A notch wear can arise at the periphery of the contact between the cutting tool and the workpiece, as a result of abrasion and oxidation due to reactions with the surrounding atmosphere. Cutting tool fractures and plastic deformations are not solely linked to wear mechanisms, but also to high compressive stresses acting on the cutting edge⁵¹. Many parameters influences how the cutting tool is worn, for example the selected cutting data, the properties of the machined workpiece and the properties of the selected insert^{53,54}.

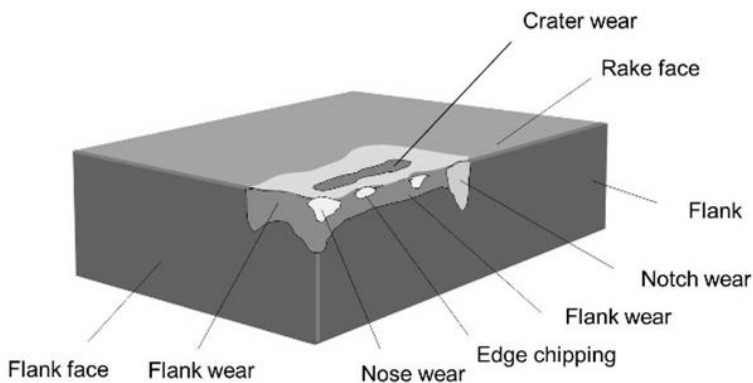


Fig. 2.6 Typical wear morphologies in metal cutting processes due to an abrasion, an adhesion, a chemical wear or a heavy load^{9,35}.

CHAPTER 3

EXPERIMENTAL

3.1. Workpieces

Six steel grades were evaluated in this thesis. Their batch compositions, their delivery state and the used designations in this study are given in Table 3.1. Specifically, soft annealed (spheroidised) bars of 90 mm in diameter and a 500 mm length were used to differentiate the machinability between similar steel grades during soft part turning (Paper II, III). Furthermore, carburised workpieces of 90 mm in diameter and 250 mm in length were used to study the active tool wear mechanisms during hard part turning (Paper IV,V). In addition, carburised middle cones of 170 mm in diameter (see Fig. 3.1) were used for studies of the machinability of the transmission parts at Scania (Paper VI). The steel grades R, M, C and UC were evaluated using laboratory scale experiments whilst the structural steel grades 280R and 280M were evaluated during industrial production.

The reference steel grades R^a and R^b are regular steels, which mean that they are typically used in automotive applications. The M-steels are treated to a calcium content of 20-60 ppm whilst having a sulfur level of 280-340 ppm, in order to improve the machinability. The clean steel grades C (20-40 ppm S) and UC (< 20 ppm S) contain a low amount of impurities which enables the extreme mechanical

Experimental

strength that is of high importance in transmission components such as gears and crown wheels. Here, the rotating bending fatigue strength of a standard and a clean steel are compared in Fig. 3.2. Further details regarding heat treatments are specified in the experimental section of each paper.

Table 3.1 Chemical composition of the steels investigated, in wt-%, Fe balanced.

Grade	Condition	In paper	C	Si	Mn	Cr	Ni	S*	O*	Ca*
R ^a	Soft annealed	II, III	0.21	0.24	0.88	0.56	0.50	280	9	-
C ^a	Soft annealed	II, III	0.20	0.24	0.60	0.53	1.69	30	5	-
UC ^a	Soft annealed	II, III	0.17	0.32	0.78	1.13	1.35	20	4	-
R ^b	Carburised	IV,V	0.22	0.22	0.84	0.56	0.52	410	9	2
M ^b	Carburised	IV,V	0.22	0.25	0.86	0.55	0.43	340	19	26
C ^b	Carburised	IV,V	0.20	0.24	0.57	0.52	1.68	40	5	2
UC ^b	Carburised	IV,V	0.18	0.34	0.75	1.14	1.40	10	4	10
280R	Carburised	VI	0.23	0.33	1.56	0.18	0.13	260	11	11
280M	Carburised	VI	0.18	0.32	1.44	0.38	0.13	280	16	53

* Contents of S, O and Ca are given in ppm.

^a Workpieces used during the laboratory experiments for a soft machining.

^b Workpieces used during the laboratory experiments for a hard machining.

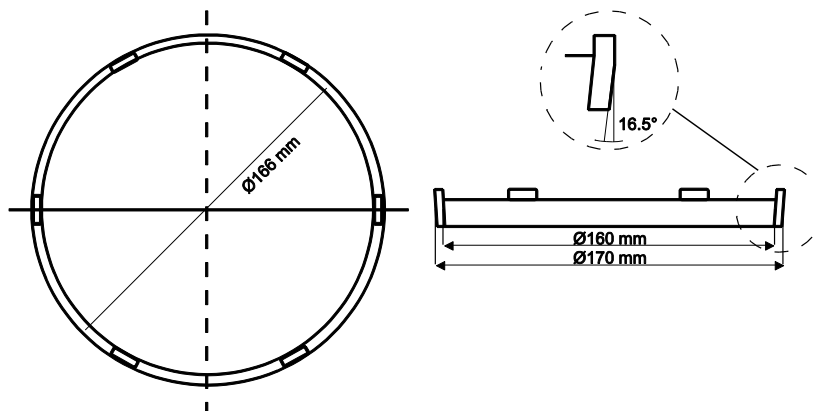


Fig. 3.1 A schematic of the carburised middle cones made of 280R and 280M⁵⁵.

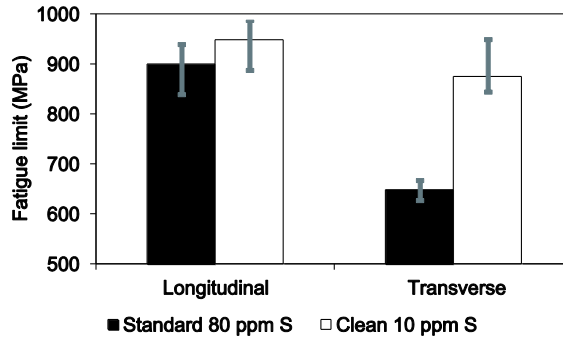


Fig. 3.2 A comparison of the fatigue limits between an ultra-clean grade and a steel comparable with an ultra-clean grade, but with a sulfur level of 80 ppm. Data are given for both the longitudinal and transverse directions¹⁰.

3.2. Cutting tools

Three different cutting tools were used in this thesis (Table 3.2). A Sandvik Coromant cemented carbide cutting tool of type CNMG120408PM GC4325 was used to determine the machinability of carburising steel grades for soft operational conditions (Paper II, III). In addition, a PCBN tool which was composed of 50 vol% of CBN and containing a binder consisting of TiCN and Al₂O₃ (made by Sandvik Coromant), was used during a hard part turning of carburised bars from the laboratory experiments (Paper IV, V). It has a 30° chamfer of a 0.2 mm width, cp. Fig. 3.3. Finally, a SECO PCBN cutting tool with the designation CCGW09T308S-01030, CBN 150 was used to study the tool wear for a gearbox production of synchronising rings (Paper VI). The grade is composed of 45 vol% CBN along with a ceramic binder of TiCN and Al₂O₃. It has a 30° chamfer of a 0.1 mm width. Figure 3.3 illustrates the key terms for the tool wear studies.

Table 3.2 Test matrix used for interrupted cutting tests.

Substrate	In paper	Binder	Macro geometry	Grade
WC	II, III	Co-based	CNMG120408PM	GC4325
PCBN	IV, V	50 vol% TiCN, Al ₂ O ₃	CNGA120408S-02030	CB7014
PCBN	VI	55 vol% TiCN, Al ₂ O ₃	CCGW09T308S-01030	CBN150

Experimental

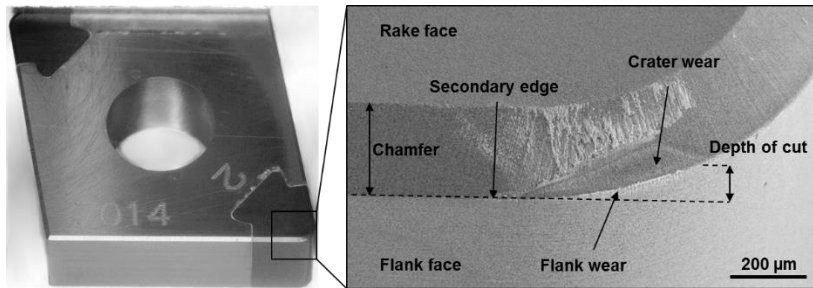


Fig. 3.3 Overview of the a) PCBN cutting tool used in paper IV,V and b) typical tool wear patterns¹⁰.

3.3. Machinability studies

The purpose of the machinability studies was to determine the influence of the microstructure and non-metallic inclusions on the cutting tool wear rate of carburising steel grades during soft and hard part turning. The approach was to employ simple machining tests and to use quantitative characterisation techniques to evaluate the underlying factors. The test series can be divided into three categories, namely chip mapping, tool life tests and interrupted tests. Most attention was paid to the tool life and the interrupted tests since the following analysis of the used cutting tools revealed important information about the active tool wear mechanisms.

3.3.1. Chip mapping

The chip mapping test was conducted to study the chip formation process of carburising steel grades under soft operational conditions. In addition, dry longitudinal turning of steel bars was performed at the cutting speeds of 200 and 300 m/min by using a Fischer CNC (computer numerically controlled) turning lathe at Sandvik Coromant. The combinations of depths of cut (0.5-5 mm) and feed rates (0.15-5 mm/rev) were used to produce chip maps with the purpose to facilitate the interpretation of the transition point from good to poor chip breakage. The Sandvik Coromant CNMG120408PM GC4325 cutting tool was used for these tests.

3.3.2. Tool life

The first tool life test was conducted to study the effect of the grain size, carbon equivalent, micro hardness, composition, size, morphology and content of non-metallic inclusions on the cemented carbide cutting tool life during soft machining (Paper II, III). A GILDEMEISTER CNC machine was used for the face turning of soft annealed bars made of steel R, C and UC. A blend made of a 5% emulsion was used as cooling media. Moreover, a feed rate of 0.3 mm/rev and cutting speeds between 280-560 m/min were used. Due to the anisotropic material properties of the investigated steel bars, the depth of cut was varied in two steps during a machining operation, namely in one cut from 2-3 mm and in the next from 3-2 mm. This procedure was repeated until a desired flank wear equal to or greater than 0.3 mm was reached or the insert was damaged by an edge fracture or a chipping. Furthermore, the machining rate that would give a 15 minute (v_{15}) of cutting tool service life was estimated by using the well-established Taylor's equation:

$$v_c \cdot T^{\alpha_T} = C_T \quad (1)$$

where α_T is a constant that describes the derivative of the logarithmic line in the Taylor plot whilst C_T refers to the extended line that crosses the x-axis, which makes it possible to estimate the theoretical cutting speed that would give 1 min tool life. Extended versions of this equation have been developed⁵⁶⁻⁵⁹, but this equation was used to get a quick indication on the machinability difference of similar grades.

The second tool life test was conducted to study the effect of the inclusion composition on the tool wear and material transfer from the chip flow to the PCBN cutting tool rake face at hard part turning (Paper IV,V). Dry longitudinal turning of bars made of steel R, M, C and UC were conducted in a CNC OKUMA LB 300-M turning lathe. The cutting data were kept constant and a feed rate of 0.1 mm/rev, a radial depth of cut of 0.1 mm and a cutting speed of 170 m/min were

Experimental

used in all tests. The test was considered ended when the cutting tool reached a flank wear equal to or greater than 0.15 mm or got damaged by an edge fracture or chippings. Previous work^{43,60} have showed that a continuous machining process are characterised by a predictable tool wear progression and has a standard deviation (σ) value below 5%. Although additional tests were performed at a 150 and a 190 m/min rate to support the findings, here, we focus only on the tests which were performed at the given cutting data.

A third tool life test was conducted at the production site of Scania with the same approach as was used in the second tool life test. It focused on the effect of the inclusion composition on tool wear and material transfer from the chip flow to the PCBN cutting tool rake face during hard part turning. The idea was to verify that the findings in Paper IV,V can be transferred to an industrial production. Therefore, an EMAG turning lathe was used to dry machine carburised middle cones made of the steel grades 280R and 280M at a feed rate of 0.24 mm/rev, a radial depth of cut of 0.15 mm, and at cutting speeds of 166-300 m/min. The tool life limiting condition in industrial production is often the generated surface roughness of the machined component rather than a defined level of flank wear. Therefore, the used tool life criterion in this test was a surface roughness of $R_a \geq 0.7 \mu\text{m}$ of the machined middle cones or at a cutting edge failure. A compilation of the performed tool life tests are given in Table 3.3.

Table 3.3 Tool life tests of the investigated steel grades.

Steel grade	Condition	In paper	v_c (m/min)	f_n (mm/rev)	a_p (mm)	Tool life Criterion*
R, C, UC	Soft annealed	II, III	280-560	0.30	2-3	$V_B \geq 0.30 \text{ mm}$
R, M, C, UC	Carburised	IV,V	170	0.10	0.10	$V_B \geq 0.15 \text{ mm}$
280R, 280M	Carburised	VI	166-300	0.24	0.15	$R_a \geq 0.70 \mu\text{m}$

* or got damaged by chippings or edge fracture

3.3.3. Interrupted tests

Machining tests with an interruption prior to the end of life were conducted for studying the initial wear mechanisms during hard part turning. The interrupted cutting tests from Paper IV,V were evaluated after the machining times of $t_1 = 3$ min and $t_2 = 12$ minutes, respectively (Table 3.4). In addition, the M-steel was tested at a higher rate of 300 m/min. The test series during an industrial production (Paper VI) were interrupted at $t=7.5$ and 16 minutes for 280R and 280M, respectively, which corresponds to about 1/12 of their respective tool life.

Table 3.4 Test matrix used for interrupted cutting tests.

Steel grade	a_p (mm)	f_n (mm/rev)	v_c (m/min)	t_1 (min)	l_1 (m)	t_2 (min)	l_2 (m)
R, M, C, UC	0.10	0.10	170	3.0	510	12.0	2040
M	0.10	0.10	300	1.7	510	6.8	2040
280R	0.15	0.24	166	7.5	1230	-	-
280M	0.15	0.24	166	16.0	2590	-	-

3.4. Characterisation

The properties of impurities and microstructure of metals can be characterised by using different types of microscopes. Today, techniques as light optical microscopy (LOM), confocal laser microscopy (CLM), scanning electron microscopy (SEM) and transmission electron microscopy (TEM) are frequently used in scientific research to visualise material features at a macro to nano level. The most suitable technique to use depends on the requested resolution and the depth of field. Resolution, or resolving power, can be described as the instrument's ability to characterise the distribution of sample inhomogeneities⁶¹ in the lateral direction, whilst the depth of field is the span of spatial positions of the sample where the image remains sharp^{61,62}.

3.4.1. Light optical microscopy

Light optical microscopy is a technique that uses the visible light and a number of lenses to map the image. Therefore, the resolution and depth of field is in the same order of magnitude as the wavelength of light, which is about 600 nm⁶³.

For metallic materials and cutting tools made of cemented carbide and polycrystalline boron nitride, the overall microstructure and tool wear can be observed with a LOM, respectively. However, a detailed analysis of, for instance, the wear of the coatings on top of the tool substrate require another microscope with a higher ability to resolve details. In this work, light optical microscopy was primarily used for flank wear measurements of the used cutting tools (SS-ISO 3685⁶⁴), chip mappings and to characterise microstructural features of the investigated steel grades.

3.4.2. Scanning electron microscopy

The scanning electron microscope (SEM) has a higher resolution and greater depth of the field than that of a LOM. Therefore, studies of cutting tool wear mechanisms and damage as well as material transfer have been carried out by using SEM. Moreover, the SEM uses an electron gun to beam electrons onto the sample surface which forces the electrons to interact with the surface. In turn, signals are generated in form of secondary electrons, backscattered electrons and elemental X-rays, from different depths of the sample. The typical limits of each signal in terms of resolution and depths of field are given in Table 3.5 and the information depths are compared in Fig. 3.4.

Surface analyse of used cutting tools (tool wear) have been a major part of this work and the technique has been used in Paper II-VI in this thesis. A SEM equipped with detectors for backscattered electrons (BSE), secondary electrons (SE), energy dispersive spectroscopy (EDS) and electron backscatter diffraction (EBSD) was used. In

addition, microstructural features as grain size and non-metallic inclusions were characterised with the same SEM techniques. For instance, by using SEM-EDS, the inclusion particle size distributions (PSD) were investigated in two dimensions (2D) on the polished surfaces of steel specimens. The investigated non-metallic inclusions were quantified automatically by using a combination of the SEM-EDS technique with the Inca Feature software and by setting the magnification to 500x. Although impurities larger than 60 μm were quantified, the set up was adjusted for small-sized impurities with an equivalent diameter of 3 to 15 microns.

Table 3.5 Different signals generated by an electron gun and their limitations in resolution and depth of field, after^{65,62}.

Detected signal	Information	Lateral resolution	Depth of field
Secondary electrons	Surface topography, compositional contrast	5-100 nm	5-50 nm
Backscattered electrons	Compositional contrast, surface topography, crystal orientation	50 nm – 1 μm	30-1000 nm
Elemental X-rays	Elemental composition, Elemental distribution	0.5-2 μm	0.1-1 μm

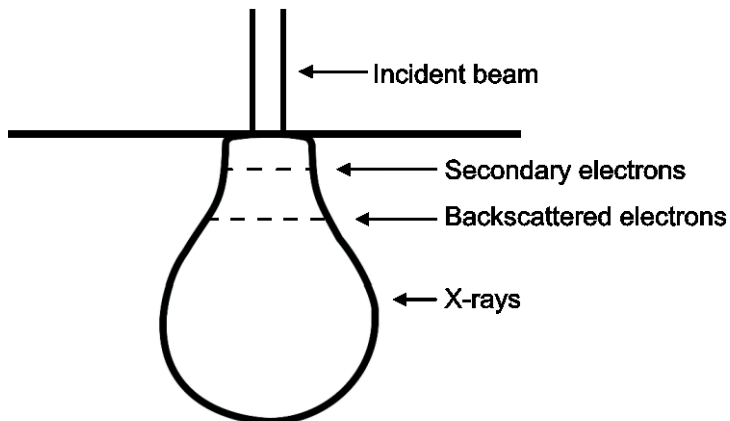


Fig. 3.4 The information depths for an incident beam, image from^{65,66}.

Experimental

The electrolytic extraction technique allows for three dimensional (3D) observations of non-metallic inclusions^{21,67,68}. During electrolytic extraction, the cathode (-) attracts positively charged metal ions whilst the metal ions collect electrons from the cathode (reduction) and are discharged as metal atoms. At the same time, the anode (+) attracts negatively charged non-metal ions which, in turn, lose their electrons to the anode (oxidation) and are discharged as non-metal atoms. These non-metal atoms can be collected on a film filter and be observed by using a SEM (see Fig. 3.5).

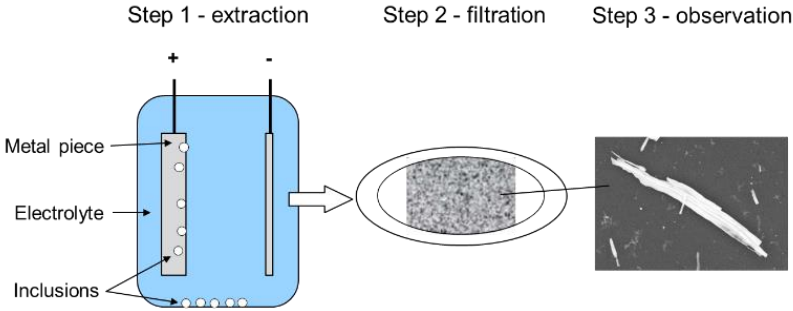


Fig. 3.5 EE-SEM allows for studying non-metallic inclusions in 3D.

In this thesis, electrolytic extraction (EE) of steel metal samples were conducted by dissolving metal samples with a 10% AA electrolyte (10% acetylacetone-1% tetramethyl-ammonium chloride-methanol) and using an electric current of 40-60 mA. During the extraction process, the weight of the dissolved steel matrix varied between 0.12 and 0.25 g. The impurities, which were not dissolved during the EE, were collected on a filter after a filtration of the solution. More specifically, a film filter with an open pore size of 0.05 to 0.4 μm was used. Thereafter, the collected inclusions were investigated on the filter surface by using a SEM-EDS. In addition, the volume fraction (N_V) of impurities in the analysed steel samples was calculated according to Eq. 2:

$$N_V = n \cdot \frac{A_f}{A_{obs}} \cdot \frac{\rho_m}{W_{dis}} \quad (2)$$

where n refers to the total count of analysed inclusions in the selected size range, A_f is the analysed film filter area after a filtration of the undissolved impurities. The parameter A_{obs} corresponds to the area of the observed steel specimen and ρ_m is the density of the steel metal piece whilst W_{dis} refers to the weight of the dissolved metal matrix during the electrolytic extraction. Also, the size of an inclusion can be described by the diameter of a spherical inclusion. For non-spherical inclusions, the equivalent diameter (d_{eq}) was calculated in accordance to Eq. 3:

$$d_{eq} = \frac{L_{max} + W_{max}}{2} \quad (3)$$

where L_{max} and W_{max} are the maximum length and width of the investigated non-metallic inclusion, respectively.

3.4.3. Confocal laser microscopy

Similarly to SEM, confocal laser microscopy (CLM) builds up an image pixel-by-pixel. The technique uses a pinhole camera with an aperture and a monochromatic light source, which can by optical sectioning through the selected depths of a sample acquire the maximum intensity for each depth. In turn, this allows for a high depth of field analysis, which makes it possible to quantify the surface profile of a sample. An Olympus OLS 3000 equipped with a 408 nm blue laser was used in this thesis to quantify the crater wear depth (K_T) of the used PCBN cutting tools (Paper IV).

3.4.4. Surface roughness

The roughness of a surface plays an important role in describing how an object, like a component in a gearbox, will interact with its surrounding parts. A rough surface is associated with large friction forces, which will cause a faster wear on its surrounding compared to smooth surfaces. In metal cutting, the generated surface roughness of a machined component is determined by the interaction between the

Experimental

cutting tool edge and the microstructure of the workpiece at the tool-workpiece interface. Gearbox components are exposed to extreme mechanical load during its service life time. Therefore, it is essential that the surface roughness of the machined components in a gearbox meets the specified tolerances. The roughness of a surface is usually characterised by using a probe to scan a specified length of a surface. The average value of the ordinates (y_1, y_2, \dots, y_n) in relation to the center line, R_a (μm), is perhaps the most common roughness value (Fig. 3.6) and can be expressed as⁶⁹:

$$R_a = \frac{1}{l} \int_0^l |y| dx \text{ } (\mu\text{m}) \tag{4}$$

where l is the length of the evaluated surface and is expressed as the x -axis in the Cartesian coordinate system.

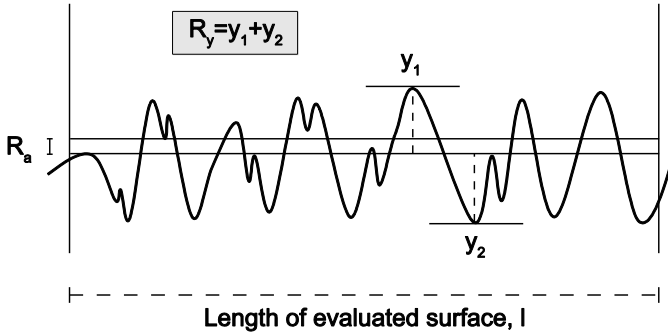


Fig. 3.6 The method to determine the roughness values of R_a and R_y .

Another common roughness value is the maximum profile height (R_y) which is the distance between the highest peak and the lowest valley of a scanned surface. In this thesis, the surface roughness (R_a) of the machined middle cones at the gearbox production of Scania was measured by using a Mahr Perthometer S2 (Paper VI).

3.4.5. Vickers hardness

The hardness of a metallic material can be described as its ability to withstand plastic deformation when an external force is applied.

Although hardness itself is not a material property it is a result from a defined test method and it is closely related to the material properties of the evaluated sample, such as the tensile strength. Hardness testing occurs by a standard procedure in accordance to the Vickers (HV), Rockwell (HR) or the Brinell (HB) method⁷⁰⁻⁷². The core of a metallic material is usually measured by the Vickers or the Brinell method whilst the case hardening depth is measured by the Vickers method. In the Vickers hardness test, an indenter of a pyramid shape with an apex angle of 136° is used to apply force at a specimen (Fig. 3.7). Due to historical reasons, the load is given in kiloponds (kp). When the indenter is removed after indentation, both the quadratic indentations are measured and the hardness is calculated. The HV value is calculated as follows:

$$HV = constant \cdot \frac{\text{indentation force}}{\text{area of indentation}} = 0.102 \cdot \frac{2 \cdot F \sin \frac{136^{\circ}}{2}}{d^2} \quad (5)$$

where F is the applied force given in Newtons, the parameter d is the mean values of the indentation's diagonals and 0.102 is a constant, a conversion factor from kp to N (1/9.81). In this thesis, Vickers hardness (HV₅, HV₁) measurements were conducted in order to characterise the core hardness of soft annealed steel grades, and the surface hardness and case hardening depth of carburised steel.

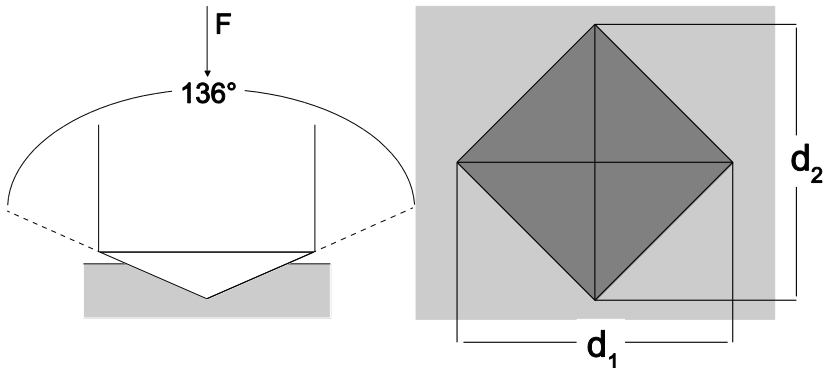


Fig. 3.7 Hardness testing according to the standard Vickers procedure²⁸.

Experimental

CHAPTER 4

RESULTS AND DISCUSSION

4.1. Inclusion modification and control

A review on today's standard systems of non-metallic inclusions in steels and the techniques for modifying them with respect to machinability and physical properties was conducted to understand their characteristics and behaviour during machining¹⁹. It was found that an improvement of the machinability by sulfur additions is perhaps the most traditional approach. Such steels are widely known as free-cutting steels⁷³⁻⁷⁷. The machinability improving effect is linked to the increased number of stress-raising particles that are active in the primary shear zone, which eases the chip formation⁷⁸. Dependent on the machining conditions, the main purposes of the modification process of MnS inclusions are usually to:

- Modify the composition and physical properties of sulfides.
- Alter the sulfide shape from rod-like to spherical inclusions.
- Decrease the sulfide size.
- Distribute the formed sulfides homogenously in the metal matrix.

As were aforementioned in Chapter 2, additions of strong sulfide formers like Ca, REM or Zr are common steelmaking praxis to modify MnS inclusions. For the Ca-treatment, it should be noted that the CaS and MnS inclusions are completely soluble with each other at the

temperatures of molten metal⁷⁹. Thus, it allows the formation of mixed (Mn,Ca)S inclusions in the liquid steel during a Ca-treatment. Consequently, the proportions of Ca:Mn and Ca:S in the steels influences the outcome of a modification and control of MnS inclusions.

Another way to improve the machinability of steel grades is by a Ca-treatment, which can result in the formation of Ca-rich oxide inclusions that acts as a protecting layer between the cutting tool and the workpiece¹². The Ca-treatment can also alter the characteristics of oxide-based inclusions of, for instance, silica (SiO₂), alumina (Al₂O₃) and magnesia (MgO), which in turn influences on the mechanical properties of a given steel grade⁸⁰. The purpose of a Ca-treatment for oxide-rich inclusions in the molten metal can be to:

- Form the relatively soft calcium-enriched alumina or silica inclusions, which can act as natural lubricants at the contacting surface between the cutting tool edge and the chip flow. Consequently, the lubricating effect may increase the cutting tool service life time.
- Form the globular calcium silicate or calcium aluminate inclusions.
- Avoid clogged nozzles during casting of steel due to the formation of alumina-rich clusters in the liquid melt^{13,81}.
- Avoid the presence of silica inclusions, which are susceptible to plastic deformation also at temperatures above 1000°C. Thus, they can increase the anisotropy of the mechanical properties of steel.

A steel grade that has been deoxidised by aluminium or silicon during steel production contain oxide-based inclusions with the compositions corresponding to zone I and zone II of the ternary phase diagram⁸², illustrated in Fig. 4.1. In addition, pure oxides like alumina and silica are extremely hard and may fracture into small fragments during rolling. The remaining yet extremely hard fragments have a decisive

impact on the mechanical strength of the steel grades. By adding calcium to the liquid steel, the composition of the inclusions moves toward zones III and IV, respectively in Fig. 4.1. Such inclusions are softer and have the advantages of having lower melting temperatures, namely about 1400-1500°C. Furthermore, they have a globular shape and improved machinability properties. Thus, calcium aluminates form instead of alumina inclusions in Al-deoxidised steels. Moreover, in Si-deoxidised steels, mullite transforms into gehlenite or anorthite⁶.

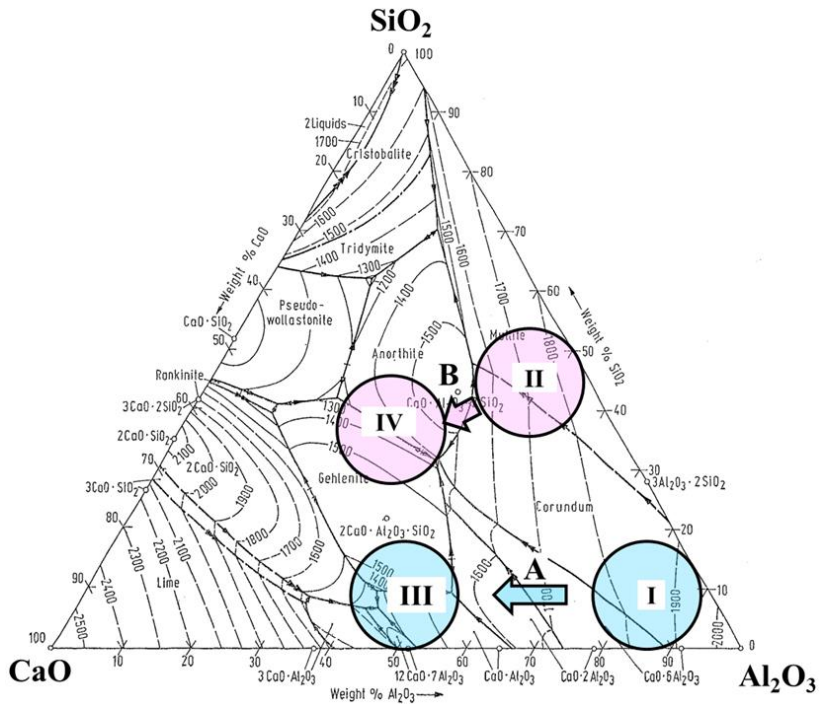


Fig. 4.1 Compositions of different oxide inclusions precipitated in aluminium (A) and silicon (B) deoxidised steel grades⁸².

4.2. Non-metallic inclusions in carburising steels

An important issue that influences the tool edge-chip contact is the presence of non-metallic inclusions in the primary shear zone.

Non-metallic inclusions can ease the chip formation process and be transferred to the rake face of the cutting tool and form a protective layer, which has a lubricating effect during machining. Therefore, the presence of non-metallic inclusions will control the cutting tool life. This is especially important at hard machining processes, where the cutting tools are expensive. The characteristics of non-metallic inclusions were studied in 2D (Paper IV) and 3D (Paper III, V, VI) to obtain an increased understanding of the underlying factors that have an influence on the machinability properties of carburising steels.

4.2.1. 2D investigations

It was found that the Ca-treated steels (modified M) were composed of Ca-aluminate based oxy-sulfides (55 - 70% Al_2O_3 , 20 - 30% CaO and 5 - 12% S) of an equivalent circular diameter (d_{eq}) of up to 30 μm^{10} . The Ca-treated steels also contained fine (Mn,Ca)S inclusions which were smaller than 15 μm . Typically, the (Mn,Ca)S inclusions were composed of 5 - 10% Ca, 50% Mn and 40 - 45% S¹⁰. The standard steel grade R contained the characteristic MnS inclusions, which were elongated to lengths greater than 150 microns. Also, the R-steel contained fine Al_2O_3 inclusions. The clean steel C contained MnS inclusions that were elongated to sizes larger than 50 μm . Furthermore, it contained a low count of (Al,Ca,Mg)O inclusions with d_{eq} values below 20 μm . Finally, it was found that the ultra-clean UC steel contained many CaS and (Al,Ca,Mg)O inclusions which were smaller than 20 μm and of a spherical shape.

The particle size distributions of sulfides, oxy-sulfides, and oxides from the evaluated steel samples from the R, M, C and UC grades were analysed to clarify the differences between the steels (Figs. 4.2-4.4). The results show that the R-steel contained a large amount of sulfides whilst the M-steel contained a large amount of sulfides and oxy-sulfides, in comparison to the clean steels C and UC. In addition, the content of oxides was low in all the samples (< 1 count/ mm^2). Furthermore, the quantified contents are given in Table 4.1.

Table 4.1 Number of non-metallic inclusions, N_A , in the tested steels.

Heat	Total (count/mm ²)	Sulfides (count/mm ²)	Oxy-Sulfides (count/mm ²)	Oxides (count/mm ²)
R	19.3	18.5	0.3	0.5
M	14.0	7.2	5.9	0.9
C	0.7	0.1	0.4	0.2
UC	1.1	1.0	0	0.1

4.2.2. 3D investigations

The SEM observations of the collected non-metallic inclusions, after EE identified the characteristics of the different types of inclusions in 3D (Table 4.2). The MnS inclusions were very thin and elongated, which indicates on a soft and ductile characteristic. Although such inclusions were most common in the resulfurised standard steel grades, they were also found in the steel samples from the Ca-treated steel grades. In addition, the plate-like (Mn,Ca)S-(Al,Mg)O inclusion type was found in the standard steels (R, 280R) and in the Ca-treated steels (M, 280M) together with the globular (Al,Mg)O-MnS inclusions. On the contrary, the clean steel C did not contain any Ca-enriched inclusions. Instead, it contained elongated MnS and globular (Al,Mg)O inclusions, which were observed both as single and mixed particles. In addition, the globular CaS and the pure (Al,Mg,Ca)O inclusions were found in the UC-steel. Overall, the MnS inclusions were found to have an elongated shape and having lengths of more than 150 μm . The Ca-enriched oxy-sulfides were less elongated and often of a more globular shape, whilst the pure oxides had the most spherical appearance of all the observed inclusions.

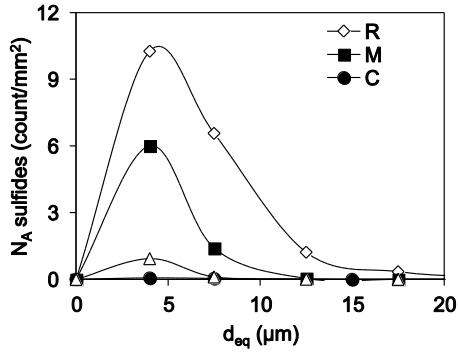


Fig. 4.2 Particle size distributions of the sulfides of the investigated steels⁸³.

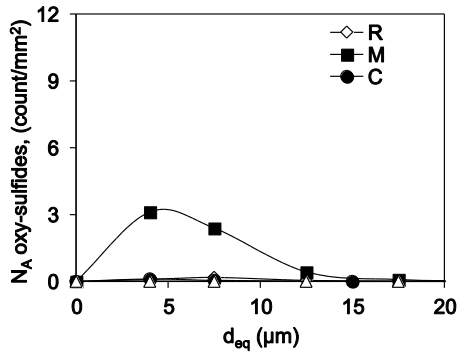


Fig. 4.3 Particle size distributions of the oxy-sulfides of the investigated steels⁸³.

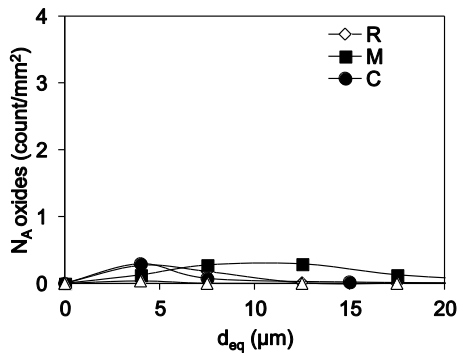
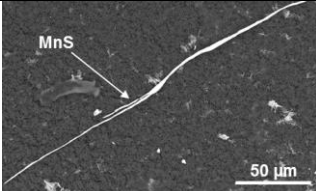
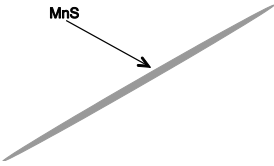
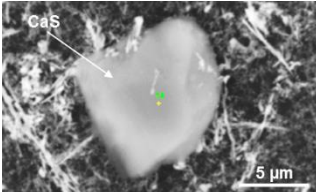
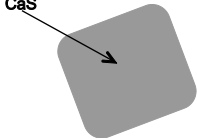
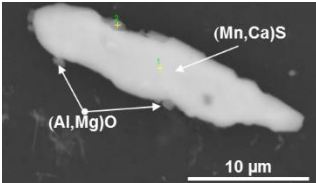
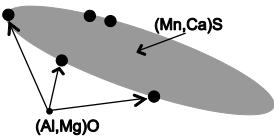
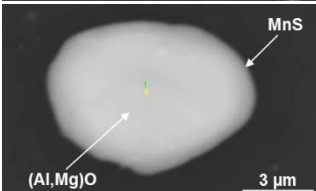
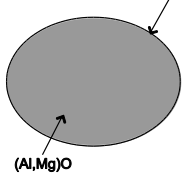
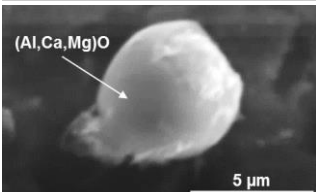
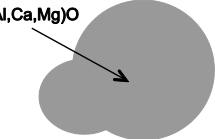
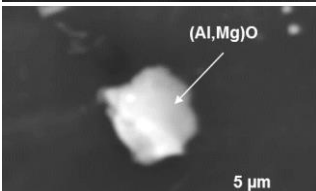
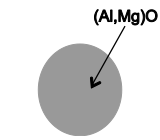


Fig. 4.4 Particle size distributions of the oxides of the investigated steels⁸³.

Table 4.2 Typical non-metallic inclusions observed in the investigated steels.

Inclusions	3D observation in the SEM	Schematic illustration
MnS 5-300 μm	 SEM image showing a long, thin, needle-like MnS inclusion. A scale bar of 50 μm is present in the bottom right.	 Schematic illustration of a long, thin, needle-like MnS inclusion.
CaS 3-10 μm	 SEM image showing a large, roughly square CaS inclusion. A scale bar of 5 μm is present in the bottom right.	 Schematic illustration of a large, roughly square CaS inclusion.
(Mn,Ca)S-(Al,Mg)O 5-60 μm	 SEM image showing an elongated inclusion with (Mn,Ca)S and (Al,Mg)O phases. A scale bar of 10 μm is present in the bottom right.	 Schematic illustration of an elongated inclusion containing (Mn,Ca)S and (Al,Mg)O phases.
(Al,Mg)O-MnS 5-20 μm	 SEM image showing a roughly circular inclusion with (Al,Mg)O and MnS phases. A scale bar of 3 μm is present in the bottom right.	 Schematic illustration of a roughly circular inclusion containing (Al,Mg)O and MnS phases.
(Al,Ca,Mg)O 2-8 μm	 SEM image showing a roughly circular inclusion of (Al,Ca,Mg)O. A scale bar of 5 μm is present in the bottom right.	 Schematic illustration of a roughly circular inclusion of (Al,Ca,Mg)O.
(Al,Mg)O 1-7 μm	 SEM image showing a small, roughly circular inclusion of (Al,Mg)O. A scale bar of 5 μm is present in the bottom right.	 Schematic illustration of a small, roughly circular inclusion of (Al,Mg)O.

4.3. Microstructural features of carburising steel

The microstructure of carburising steel grades are typically consisting of a ferritic-perlitic structure⁸⁴⁻⁸⁶, sometimes with islands of bainite⁸⁷, as is exemplified in Fig 4.5. The microstructure of the soft annealed carburising steels was investigated (Paper II, III) to enable a correlation to their behaviour during soft machining. It was found that the spheroidised cementite (Fe_3C) was precipitated inside the ferrite ($\alpha\text{-Fe}$) grains (Fig. 4.6). In addition, the crystallographic orientation and size of the same steels were characterised by using EBSD (Fig. 4.7). The grain size of the investigated samples varied from about 8 to 11 μm , where the clean steels C and UC had the smaller grain sizes.

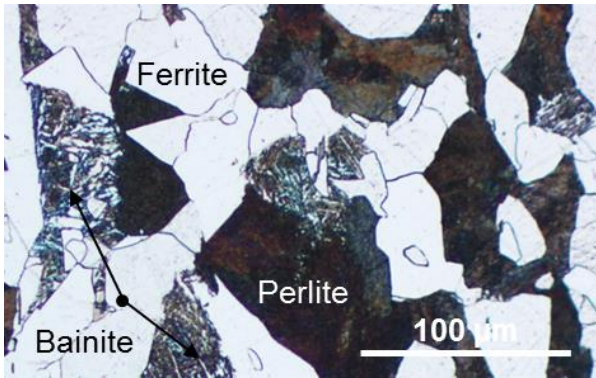


Fig.4.5 Typical microstructure of carburising steel grades.

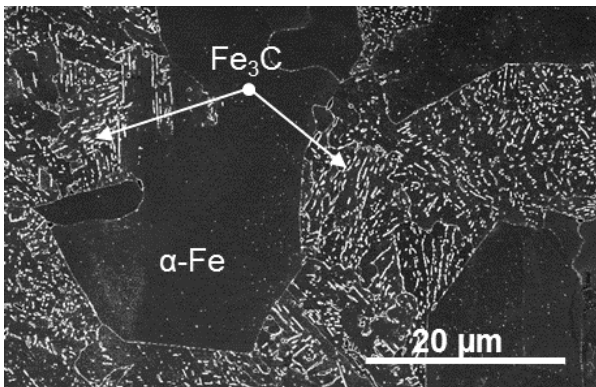


Fig.4.6 Spheroidised Fe_3C particles in the metal matrix of carburising steels.



Fig.4.7 Typical orientation and size of the grains in the investigated steel grades.

The results show that the corresponding hardness at the position of the half radius of the reference grade R (149 HV) had a 10-15% lower hardness value than the clean steels C (165 HV) and UC (171 HV), as given in Table 4.3. Since the hardness is closely related to the energy needed to produce chips during metal cutting, one can expect a longer cutting tool life time of the standard steels compared to the clean steels during soft machining.

Table 4.3. Microstructural characteristics of carburising steel grades for operational soft conditions.

Steel grade	Carbon content (wt-%)	Average grain size, D_G (μm)	Hardness at $\frac{1}{2}$ radius, HV _{0.5R} (HV ₅)
R	0.21	11.0 ± 0.3	149 ± 4
C	0.20	9.4 ± 0.5	165 ± 6
UC	0.17	8.2 ± 0.3	171 ± 1

4.4. The machinability of carburising steels in soft condition

The ability of the R, C and UC grades to form chips during soft part turning was studied (Paper II) for the cutting speeds of 200 and 300 m/min. The results show that the standard steel R was able to form acceptable (short and arc-like) chips for a wider range of cutting data combinations (feed rate and depth of cut) than the clean steels, as

Results and discussion

indicated by the section of good chip formation in Figs. 4.8 and 4.9.

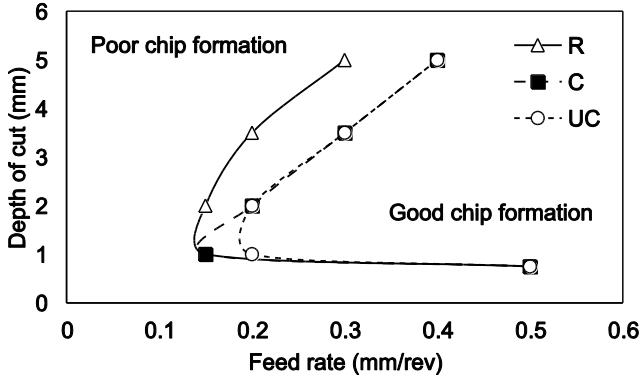


Fig. 4.8 Chip map diagrams after soft machining of R (a), C (b) and UC (c) steel grades, at a speed of 200 m/min.

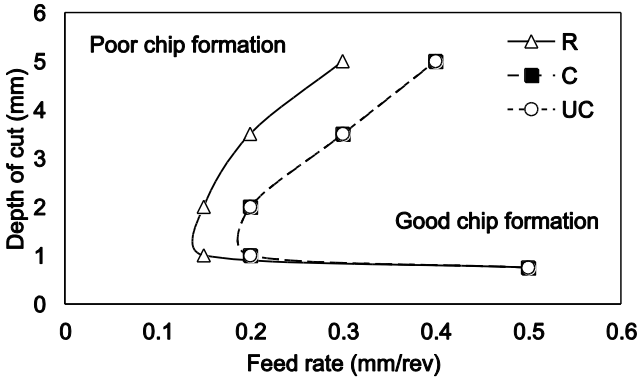


Fig. 4.9 Chip map diagrams after soft machining of R (a), C (b) and UC (c) steel grades, at a speed of 300 m/min.

Only minor differences between the chip breakability of the steel grades C and UC was found. Overall, the method can be used for machinability differentiation of similar steel grades. Here, chip mapping is a conventional method that has been frequently used to evaluate the chip formation process during metal cutting^{88,89}. Although it is not a new method, it has been proven to be useful in this work.

In the same study⁹⁰, the cutting tool life of the tested steel grades R, C and UC was evaluated during soft part turning. The study showed that the reference steel grade generated a longer service life time of the cutting tool compared to the clean steels. In addition, the estimated cutting speed that results in 15 minutes of tool life (v_{15}) was 436, 376 and 353 m/min for R, C and UC, respectively (cp. Fig. 4.10). Beside the lower v_{15} value of UC, the large scatter of the obtained tool life values for the different cutting speeds indicate a reduced machinability compared to the steel grades R and C. The low scatter of the tool life values of R indicate on a more robust machining process, which is of high importance during an industrial production.

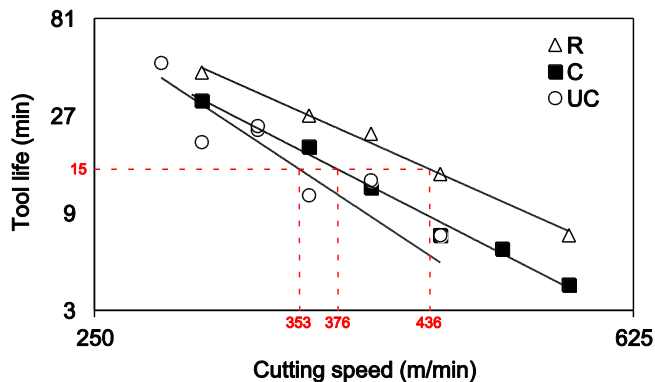


Fig. 4.10. Taylor diagram of the investigated steels at $f_n=0.3$ mm/rev and $a_p=2-3$ mm⁹⁰.

The obtained cutting tool life values were empirically correlated to the average grain size of the steels and it was found that the tool life increased with an increased average grain size (Fig. 4.11). It can be explained by the fact that a small average grain size is associated with a high tensile strength, in accordance to the Hall-Petch relation⁹¹⁻⁹³, see Eq. 6, where σ_y represents the contribution of friction-free stress from grain boundaries and k_y is a material dependent constant whilst D_G is the average grain size of the steel grade⁹³. Therefore, a steel grade with a small average grain size consumes a larger amount of energy during machining. Thus, this leads to a reduced tool life.

$$\sigma_y = \sigma_0 + k_y D_G^{-\frac{1}{2}} \tag{6}$$

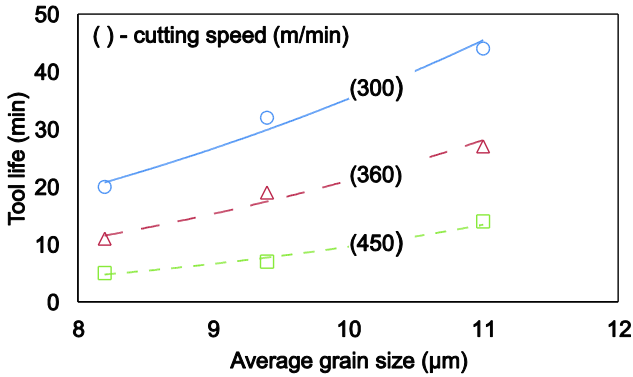


Fig. 4.11 The link between the average grain size and the cutting tool life⁹⁴.

Also, it was found that the cemented carbide cutting tool life depends on the volume fraction of non-metallic inclusions of the carburising steel grades (Fig. 4.12). It was also found that the tool life increased with increased sulfur contents. This result was expected as published work have reported on similar findings⁹⁵. An increased content of impurities leads to an increased amount of stress-raising particles at the tool-chip interface which eases the chip formation³³.

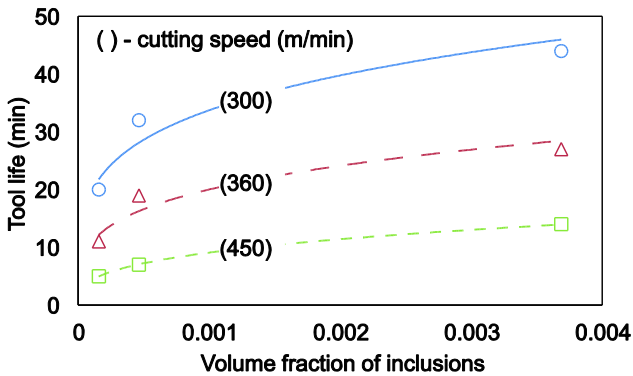


Fig. 4.12 The link between the volume fraction of inclusions and the cutting tool life⁹⁴.

4.5. The machinability of carburising steels in hard condition

Hard part turning of carburised steel was conducted at a laboratory and an industrial scale to study the PCBN tool wear and the material transfer from the workpiece to the rake face of a cutting tool (Paper IV-VI).

The results show that the machinability was improved, specifically, Ca-treated steel show a superior machinability (longer tool life) in comparison to the standard and the clean steels. A doubled tool life (102 min) was obtained compared to the standard steel (49 min) and an about tripled tool life was obtained compared to the clean steels (32-39 min), as shown in Fig. 4.13. The standard steel grade (R) failed because of an edge fracture whilst the other steel grades met the tool life criterion of a 0.15 mm flank wear.

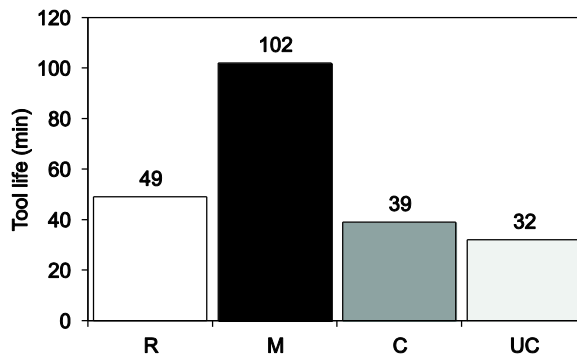


Fig. 4.13 Cutting tool service life time of the investigated steel grades. ($f_n = 0.1$ mm/rev, $a_p = 0.1$ mm and $v_c = 170$ m/min)¹⁰.

The tested PCBN edges display a balanced wear pattern of a flank and a crater wear at the end of tool life, as seen in Fig. 4.14. This was true except for the reference steel grade R which caused edge fractures (Fig. 4.14a). The steel grades C and UC resulted in a larger crater wear than the high sulfur steels R and M, and the corresponding crater depth at the end of tool life of the used PCBN edges was 36, 11, 48 and 40 μ m for the R, M, C and the UC steel, respectively. Note the very small crater wear of the M-steel in Fig. 4.14b. Furthermore, a ridge

Results and discussion

formation was detected in the PCBN crater after hard part turning the modified Ca-treated steel (Fig. 4.14b) whilst the clean steels generated edge chippings (see Figs. 4.14c and d). The flank wear developed faster for the C and UC grades in comparison to the R and M grades, as seen in Fig. 4.15. Although the tendencies were not as pronounced as those at tool life, the results indicated that the clean steels caused a more severe crater wear and a more frequent edge chipping also on the used cutting tools from the interrupted tests (Paper IV).

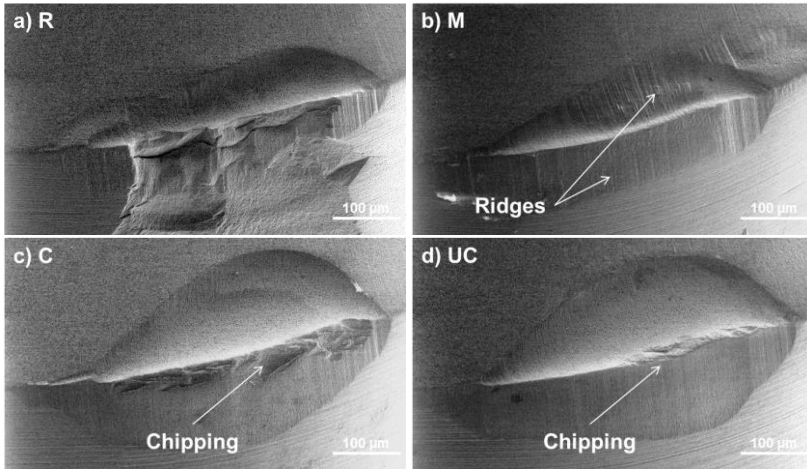


Fig. 4.14 The PCBN edges imaged by SEM at their tool life. a) R (t=49 min) b) M (t=102 min) c) C (t=39 min) and d) UC (t=32 min)¹⁰.

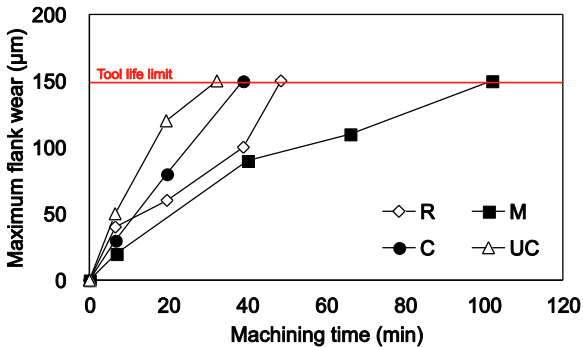


Fig. 4.15 Flank wear measured during the tool life tests ($f_n = 0.1 \text{ mm/rev}$, $a_p = 0.1 \text{ mm}$ and $v_c = 170 \text{ m/min}$)¹⁰.

The machinability of the Ca-treated M-steel was as superior during the industrial production as well as in the laboratory experiments. The results show that the M-steel (280M) had a more than doubled cutting tool life (38 min) compared to the reference steel 280R (18 min) at a cutting speed of 166 m/min (Fig. 4.16). Moreover, the tool life criterion of $R_a \geq 0.7 \mu\text{m}$ was met for the R-steel whilst the M-steel caused distortions of the machined parts and tool edge chippings due to its extended service life time. From the surface roughness measurements, it can be observed that the R_a value of 280M levels out below $0.6 \mu\text{m}$ whilst the R_a value from the 280R-steel increases continuously until it reaches the tool life criterion of $0.7 \mu\text{m}$ (Fig. 4.17).

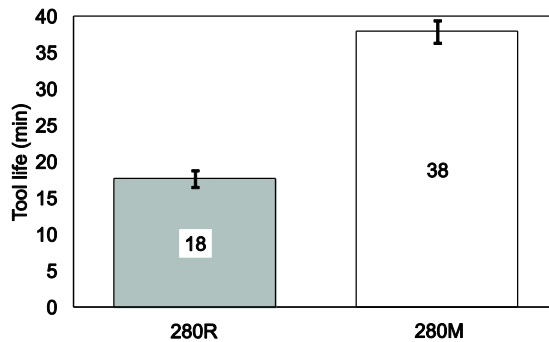


Fig. 4.16. Tool life of 280R and 280M. ($f_n=0.24 \text{ mm/rev}$, $a_p=0.15 \text{ mm}$, $v_c=166 \text{ m/min}$)⁵⁵.

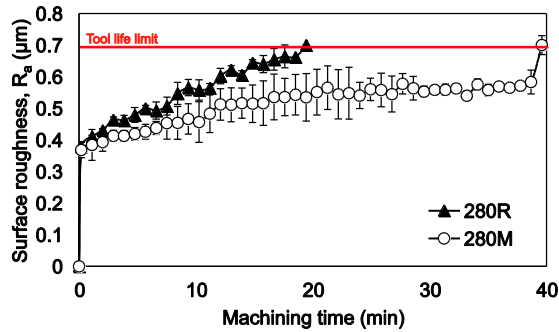


Fig. 4.17 The generated surface roughness during industrial production of transmission products. ($f_n=0.24 \text{ mm/rev}$, $a_p=0.15 \text{ mm}$ and $v_c=166 \text{ m/min}$)⁵⁵.

The tool life tested PCBN edges from the industrial production

Results and discussion

indicates on similar wear mechanisms as those which were observed during the laboratory tests. Both the R and M steels developed a balanced wear mode consisting of a flank and a crater wear (Fig. 4.18), even though edge chippings also were detected. It is important to point out the more pronounced PCBN flank wear after cutting in the M-steel, which corresponds to its prolonged service life. Also, during the laboratory tests, a characteristic ridge formation was developed in the chip-exit area of the rake face crater after a completed hard turning of the M-steel (see Fig. 4. 14b). The same wear pattern was observed in the PCBN rake face crater after machining the R (280R) and M (280M) steels during an industrial production, cp. Fig. 4.18. Overall, industrial production trials verified that the M-steel has a superior machinability compared to the standard steel (R).

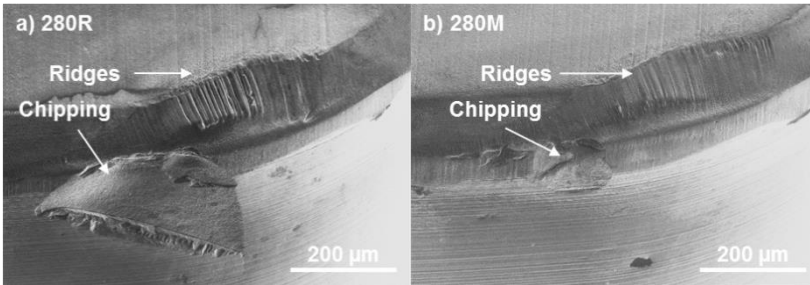


Fig. 4.18. The PCBN edges imaged at the end of the tool life time. a) 280R (t=18 min), b) 280M (t=38 min). (SEM-SE)⁵⁵.

4.6. Material transfer during hard part turning

The material transfer from the chip flow to the rake face of the used PCBN cutting tools were studied in order to understand the role of non-metallic inclusions on the tool wear during hard part turning (Paper IV-VI). The focus was on the link between the inclusion composition of carburising steel grades and the active wear modes. It was found that a layer of workpiece material (Fe) was transferred to the PCBN cutting edge after turning of the clean steels. The transferred layers were enriched at the exit region between the chip flow and the PCBN crater (Fig. 4.19). Furthermore, the edges that travelled through

the M-steels showed very little transfer of workpiece material (Fig. 4.19b), whilst the reference steel R generated a burr-like formation of steel remnants along the cutting edge (Fig. 4.19a).

EDS analyses of the M-steel rake face crater detected deposits enriched in Mn, Ca and S as is exemplified in Fig. 4.20. The zone enriched in Mn and S had a characteristic elongated shape, which were located at the depth of the crater in parallel to the cutting edge. Furthermore, the EDS revealed that a low concentration of calcium was distributed rather uniform in the rake face crater, as seen in Fig. 4.20. Although some deposits enriched in Mn, Ca and S were detected, this tendency could not be clearly observed after a machining of the reference steels. Moreover, a hard part turning of the M-steels generate enrichments of Al, O, Ca, Mn and S, which were observed in the ridge formations of the PCBN rake face crater, see Fig. 4.21. Correspondingly, it is suggested that the formation of PCBN ridges is the result of a contact between the PCBN rake face, and the deposited slag layers of (Mn,Ca)S and (Ca,Al)(O,S). From the inclusion studies of Paper IV, it was found that the slag composition correlates to the inclusion content of the M-steels, which were composed of (Mn,Ca)S inclusions (5-10% Ca, 50% Mn and 40-45% S) and Ca-aluminate rich oxy-sulfide inclusions (55-70% Al_2O_3 and 20-30% CaO and 5-12% S).

Except from very small enrichments, no slag layers could be seen on the PCBN rake face after turning the standard and the clean steels. Thus, it is established that the transferred layers enriched in (Mn,Ca)S are formed by a Ca-treatment. These layers are believed to be relatively stable. Thus, they are able to protect the contacting surface of the PCBN edge from the chip flow. Furthermore, a Ca-treatment of molten steel promotes the formation of less elongated (Mn,Ca)S inclusions^{33,78,96}, which is supported by the findings in this study (Table 4.2.). Ca-rich sulfides have a higher hot-hardness than pure MnS inclusions⁹⁷. Thus, it is believed that pure MnS inclusions are not stable enough to form protective layers at elevated temperatures.

Results and discussion

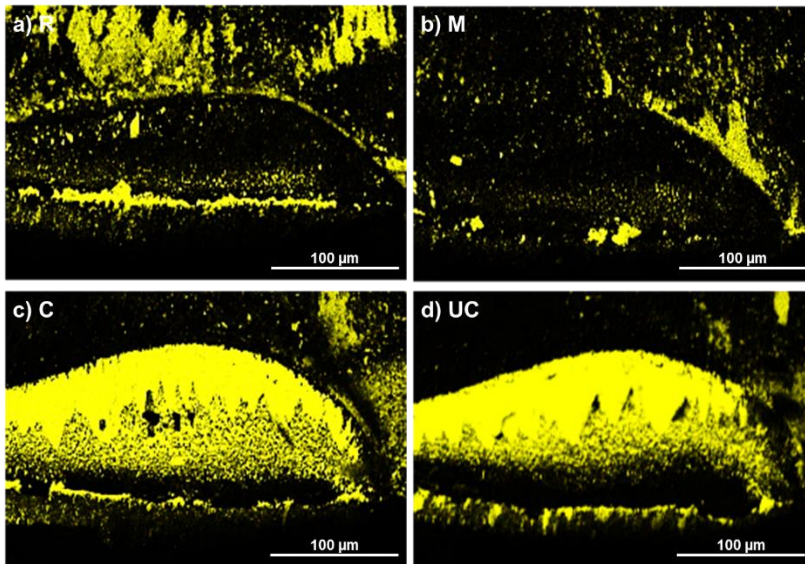


Fig. 4.19 EDS-maps of Fe in the crater and edge area after turning tests interrupted at a 2040 m cutting distance, obtained from the edges shown in Fig. 4.14¹⁰.

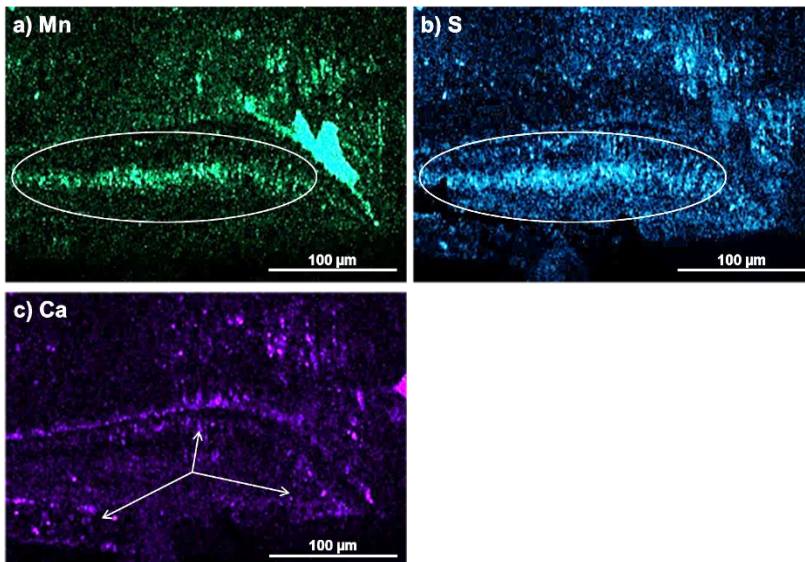


Fig. 4.20 EDS-maps of Mn, S and Ca, respectively in the crater and edge area of the M-steel after the cutting tests were interrupted at a 2040 m distance¹⁰.

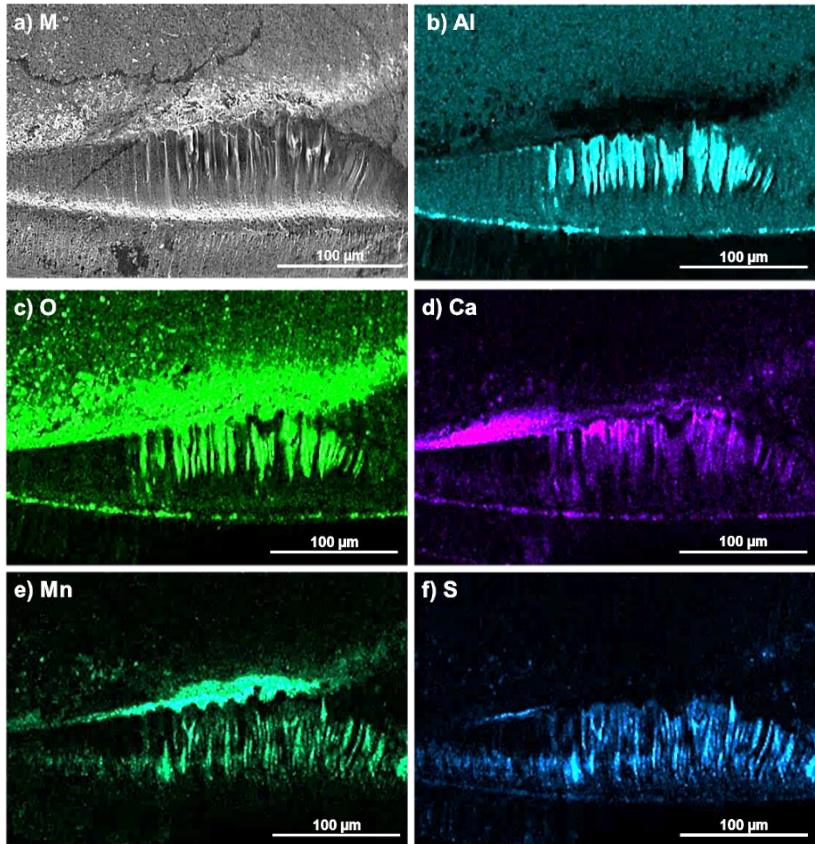


Fig. 4.21 Electron micrograph (a) and EDS-maps of Al, O, Ca, Mn and S, respectively, on the tool edge after cutting tests using the M-steel and using a 300 m/min rate¹⁰.

Steel from the chip flow tends to adhere and to accumulate at surface irregularities. If the temperature becomes high enough at the tool edge-chip interface, layers of workpiece metal or protective deposits can be transferred to the cutting tool. In this study, it was found that the steel constituents were transferred into different zones of the cutting edge (Fig. 4.22). Along the cutting edge (Zone A), remnants from the chip flow was detected (Fe and O) whilst Ca-enriched deposits were found near the crater depth (Zone B) and in the upper part of the rake face crater (Zone C). Similar findings were presented

by Brion et al. which supports the current results⁹⁸.

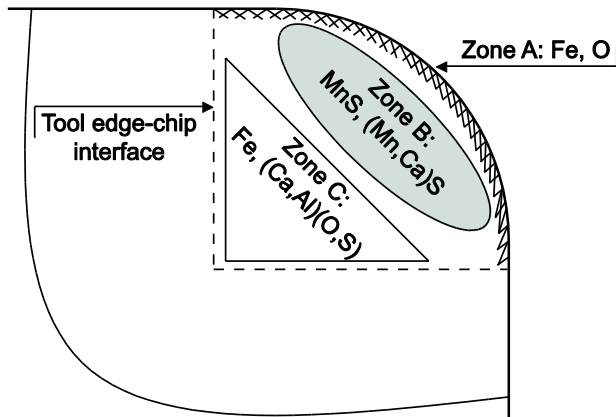


Fig. 4.22 Schematic drawing of the tool edge-chip contact zone and the distribution of the transferred Fe, O, Al, Mn, Ca, and S from the workpiece^{55,98}.

4.7. The role of non-metallic inclusions

This thesis has shown that the superior machinability of the Ca-treated, machinability improved steels (Figs. 4.13 and 4.16) is linked to the formation as well as the stability of protective slag layers that are built up on the contacting surface of the PCBN edge (Figs. 4.20 and 4.21). It is proposed that the presence of slag layers composed of workpiece atoms are essential to minimise the chemical degradation of the tool edge due to a contact with the chip. During this process, sulfur minimises the material transfer from the chip flow, whilst Ca-treated impurities have a stabilising effect on the protective deposits of slag layers. Without a protection, cutting tool edges are exposed to adhesive Fe-rich features that attack and penetrate through the PCBN contact surface and cause a depletion of the CBN grains⁹⁹.

Overall, the M-steels generated an about doubled to tripled cutting tool service life time compared to the standard and the clean steels, respectively. Also, the reduced wear rate of the M-steel can be used for increased metal removal rates, which is of high importance for

industrial production where cycle time of machining processes is an everlasting challenge. The quantified machinability differences between the steel grades in hard part turning are similar to what have been reported in previous studies of M-steels^{12,100}. For example, Väinölä et al. highlighted the machinability of steel grades comparable to those of the R-steel and the M-steel for a soft condition. In that study, it was found that an about 40% higher cutting speed could be used for the M-steel to get the same tool life as for the R-steel¹⁰⁰.

The studies of non-metallic inclusions which were summarised in Paper III-VI made it possible to detect correlations between inclusion characteristics and machinability. It was found that the volume fraction of non-metallic inclusions of the Ca-treated steels (M) was about 30% lower than that of the standard steels (R), whilst the inclusion morphology and size ranges were comparable. Thus, the underlying effect of the machinability improved M-steels is linked to the inclusion composition rather than the content and size of non-metallic inclusions. Still, although the clean steels C and UC had a content of non-metallic inclusions which were about 95% lower than the standard steels, machining C and UC only resulted in a 20-40% reduced tool life.

4.8. Comparison between standard steels and clean steels

It has been clarified that the clean steels generate a rapid tool wear degradation and a worse chip formation compared to the standard steel grades. The poor machinability of the clean steels is linked to their low content of non-metallic inclusions. A low content of non-metallic inclusions increases the risk for tool wear degradation due to abrasion, adhesion and diffusion-induced chemical depletions.

The major difference in terms of generated tool wear pattern among the machined steel grades is the significantly more advanced crater wear of the clean steels compared to the standard steel grades (Paper IV-VI). It is caused by the transfer of workpiece material (Fe)

Results and discussion

from the chip flow to the rake face crater of the cutting tool. The transferred workpiece material (Fe) has a strong affinity to CBN and can by diffusion penetrate through the tool edge surface and deplete the CBN grains. This phenomenon is promoted by a high temperature, which is common during machining of hardened steels¹⁰¹. Angseryd et al. reported that the material transfer of Fe-rich compounds increased with a decreased sulfur content, which corresponds to the findings in this thesis⁹⁹.

4.9. The business case of the M-steel

The improved machinability of the M-steels offers an attractive potential in saving money. Therefore, a cost-save calculation was conducted to exemplify the cost-saving potential of M-steels. The annual production volume of middle cones for synchromesh gearboxes is roughly 200 000 parts and the tooling cost per piece is about 42 Euro. If it is assumed that an about doubled tool life of the M-steel as compared to the reference steel was obtained, it would lead to an annual tooling cost-saving of 50% (Fig. 4.23). Thus, the M-steel has the potential to further reduce the manufacturing cost per produced piece during industrial production. However, before implementing an M-steel, its behaviour through the complete manufacturing route must be mapped to avoid unexpected downtime.

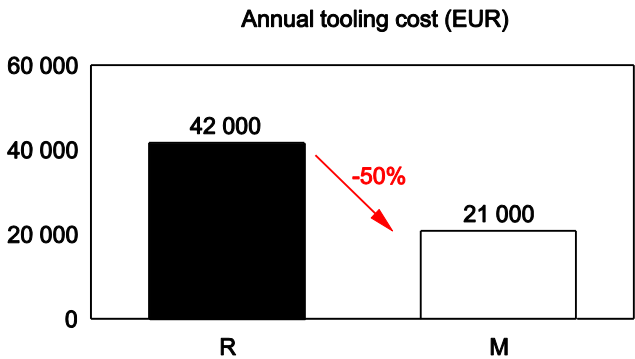


Fig. 4.23 A cost-save calculation based on the prolonged service life of the M-steels⁵⁵.

CHAPTER 5

CONCLUDING DISCUSSION

A review was conducted (Paper I) in order to map the most common impurities that can be found in various steel grades. Most attention was paid to the characteristics of different non-metallic inclusions and their behaviour in the primary shear zone during metal cutting. In addition, the possibilities for a modification and control of non-metallic inclusions were investigated as it links to the quality of the final steel piece such as transmission components of a gearbox. The study resulted in an overview and a general description of the physical behaviour of different non-metallic inclusions. Overall, the results highlighted the possibilities and challenges to modify existing steel grades for an improved machinability. Thereby, the limitations and expectations of the following machinability studies of carburising steel grades could be defined. Moreover, the results can be used as information for metallurgical considerations during the modification of current steel grades and the development of new steel grades.

Previous, it was uncertain if it was even possible to differentiate between the machinability of similar steel grades, having only minor differences in microstructure and steel composition. Therefore, the conventional tool life and chip mapping tests were conducted (Paper II) by using three similar carburising steel grades to investigate their differences in tool wear and chip formation during soft part turning. The results show that the used methods are able to

Concluding discussion

differentiate the machinability between these steels. This verification allowed for further machinability evaluations of steel grades that are composed of different contents and types of impurities. In addition, the obtained results show that the investigated steel grades are able to correlate its microstructural features and content of non-metallic inclusions to its machinability properties (Paper II-V). For instance, empirical relations between the grain size, micro hardness and volume fraction of non-metallic inclusions to the machinability was found. Overall, the results highlight information that can play an important role during steelmaking.

Previous work have evaluated the characteristics of transferred layers of workpiece material to the cutting edge during soft and hard machining operations^{32,33,96,102}. However, the effects of the steel cleanliness and the inclusion composition on the tool wear mechanisms during hard part turning have not been clarified. In this study (Paper IV, V), the characteristics of the non-metallic inclusions of a standard, a Ca-treated and two clean steels were evaluated and linked to the active degradation mechanisms of cutting tools. The results show that Ca-treated steels alloyed with sulfur are able to form protective slag deposits composed of (Mn,Ca)S and (Al,Mg)O-(Mn,Ca)S. Such inclusions are believed to have a lubricating effect at the tool edge-chip interface. As a result, hard machining Ca-treated steels generated a less pronounced rake face crater. This corresponds to an increased tool life in the order of 100-200% as compared to the standard and the clean steels. Overall, the content and the composition of non-metallic inclusions were found to play a vital role during hard machining of carburised steel grades. These findings were verified during the industrial production of transmission products at Scania (Paper VI). The improved machinability of Ca-treated steels are applicable for a wide range of steel components, where inclusion induced fatigue is a low risk. The increased service life time of the cutting tools is due to Ca-treatment of steels which allows for significant cost-savings in terms of tooling

costs and productivity. Therefore, to implement Ca-treated steel grades at the automotive production of Scania would have a great economic impact, both locally and globally. Finally, a summary of the conducted studies are given in Table 5.1.

Table 5.1 Overview of the main topics that are discussed in the thesis.

Paper	Study	Results	Application
I	The effect of different non-metallic inclusions on the machinability of steels	General description of the behaviour, and characteristics of non-metallic inclusions	Metallurgical possibilities to modify existing steel grades for desired machinability
II	The effect of steel cleanliness on the machinability of carburizing steel	Methods to differentiate the machinability of similar steels during soft machining	Laboratory scale experiments and development of industrial production
III	The influence of microstructure and NMI on the machinability of clean steels	Correlations between microstructural features and inclusion characteristics to machinability measures	Input to metallurgical aspects for consideration during steel the development of steel grades
IV	The effect of inclusion composition on tool wear	Correlations between inclusion characteristics in 2D and the tool wear during hard part turning	Development of cutting tool and steel grades and for optimisation of the industrial production
V	Effect of different inclusions on machinability of 20NiCrMo steels	Correlations between inclusion characteristics in 3D and the tool wear during hard part turning	Development of cutting tool and steel grades and for optimisation of the industrial production
VI	Steel characteristics and their link to tool wear in hard part turning	Correlations between steel characteristics and cutting tool life during industrial production of transmission products	Cost-save analyse for optimised industrial production, locally and globally

Concluding discussion

CHAPTER 6

CONCLUSIONS

The vision of this thesis is to study how it is possible to obtain optimised workpieces in metal cutting processes during industrial production. Specifically, the work aimed to increase the understanding between the steel characteristics and their link to the chip breaking and tool wear during metal cutting. Since there is an everlasting need to increase the production rate, whilst maintaining a high quality of the finished parts, the future production will continue to require extreme demands on the quality of workpieces. If the emphasis is focused on the workpiece, it should be possible to obtain a robust manufacturing. Therefore, the challenge for future steel metallurgists is to develop high performance grades with optimised *combined* properties of an excellent machinability together with an outstanding mechanical strength.

From the work summarised in this thesis, the following conclusions can be made:

- I. The machinability of a standard carburising steel grade for a hard condition is significantly improved by a Ca-treatment (M-treated). Also, the improved machinability of the M-steels offers an attractive potential in saving money. Specifically, the field study at Scania showed that it is possible to reduce the annual tooling cost with about 50% for some transmission products.

Conclusions

- II. The superior machinability of the M-steel is linked to the formation of lubricating slag layers of (Mn,Ca)S and (Ca,Al)(O,S) inclusions, which are formed on the rake face during the machining operation.
- III. It is proposed that the presence of slag layers composed of atoms from the workpiece are essential to minimise the chemical degradation of the PCBN tool edge due to a contact with the chip. During this process, sulfur minimises the material transfer from the chip flow, whilst Ca-treated impurities are believed to have a stabilising effect on the protective deposits of slag layers. Without a protection, the PCBN edges are exposed to adhesive Fe-rich features that attack and penetrate through the PCBN contact surfaces and cause a depletion of the CBN grains.
- IV. A more advanced crater wear was caused by the clean steels compared to the standard steel grades. It is explained by the increased degree of workpiece material transfer (Fe) from the chip flow to the rake face crater of the cutting tool. The transferred workpiece material (Fe) has a strong affinity to CBN and can by diffusion penetrate through the tool edge surface and deplete the CBN grains.
- V. Steel from the chip flow tends to adhere and to accumulate at surface irregularities. If the temperature becomes high enough at the tool edge chip interface, layers of workpiece metal or protective deposits can be transferred to the cutting tool. It was shown that the steel constituents were transferred into different zones of the cutting edge. Along the cutting edge, remnants from the chip flow was detected (Fe and O), whilst Ca-enriched deposits were enriched near the crater depth and in the upper part of the crater.
- VI. It was possible to differentiate between the machinability of similar steel grades by using the conventional machinability tests of chip mapping, tool life and Taylor diagrams (v_{15}). Even though there were only small differences in microstructural

features, it was possible to separate the machinability performances for the studied steel grades. In comparison, the chip map test is the quicker method whilst the tool life test and to generate Taylor curves are more accurate.

- VII. Non-metallic inclusions can be modified in order to alter the physical properties of steel. With emphasis on machinability, the purpose is to ease the chip formation and to form slag layers that protects the cutting tool from degradation during machining. For this purpose, the most common steelmaking praxis is to add sulfur, calcium or rare earth metals to improve the machinability properties.
- VIII. It was possible to determine the 3D characteristics of non-metallic inclusions based on the SEM observations after electrolytic extraction of steel samples. MnS inclusions were elongated to lengths more than 150 μm , whilst fine ($< 10 \mu\text{m}$) CaS inclusions were found to have a globular shape. Furthermore, (Mn,Ca)S-(Al,Mg)O inclusions were observed as plates which could be up to 60 μm in length. The globular (Al,Mg)O-MnS inclusions consisted of a oxidic core, which was surrounded by a thin rim of MnS. Finally, the pure oxides were usually found to be very small ($<10 \mu\text{m}$) and to have a globular shape.
- IX. Overall, the empirical findings showed that the cutting tool life increased with an increased average grain size and volume fraction of non-metallic inclusions.

Conclusions

CHAPTER 7

FUTURE WORK

The overall performance of a steel grade is associated to its content of defects and impurities. Recent efforts have led to the development of new steel grades with very low levels of non-metallic inclusions. These so called clean steels are characterised by an extreme fatigue strength and impact toughness. However, clean steels are often correlated with a poor chip breakability and a rapid degradation of cutting tools, which make them less attractive for manufacturing industries. Therefore, the challenge of future metallurgy is to develop high performance steels with an improved and balanced *combination* of properties of a high mechanical strength and a high machinability, as is illustrated in Fig. 7.1.

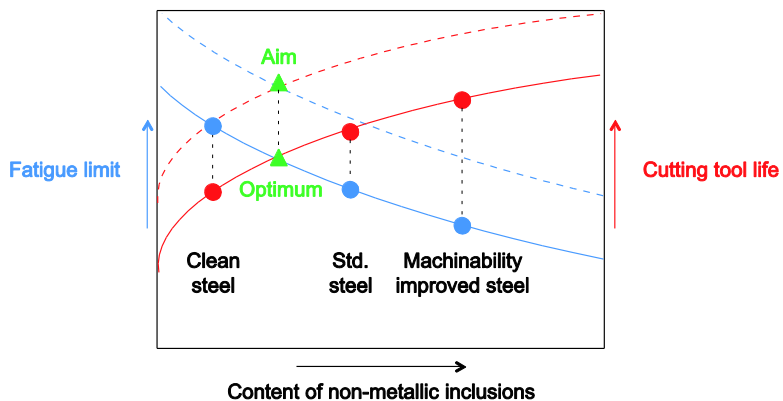


Fig. 7.1 A schematic diagram that illustrates that the challenge of future metallurgy is to develop high performance steels with improved combined properties.

Future work

One way to approach this metallurgical challenge may be to transform a small amount of large non-metallic inclusions into many but small ones, which have a desired composition and shape. Specifically, their composition should be similar to those of the (Mn,Ca)S and (Al,Mg)O-(Mn,Ca)S inclusions that were observed in this work. For this purpose, alloying additions of rare-earth metals (REM) of a carburising steel with a low content of non-metallic inclusions is suggested. For example, a 20NiCrMo7 steel could be used to control the size, shape and hardness of its non-metallic inclusions. The objective is to provide tougher steels that has optimised machinability properties. Thus, they may enable lighter constructions and thereby meet the environmental demands of the future. From the perspective of the end-user industries, it is important that the mind set allows for a serious testing and an implementation of new steel grades to take an advantage of the optimised workpieces.

This thesis has proven that Ca-treated, machinability improved (M) steel grades have a superior machinability compared to the standard steels and the clean steels. However, the conclusions are based on turning of workpieces for soft and hardened conditions. To fully approve the M-steels in an industrial production, its machinability must be mapped throughout the complete manufacturing route. More specifically, its behaviour during other machining processes such as milling, honing, shaping, drilling and grinding must be evaluated. In addition, its behaviour during a number of heat treatments must be clarified to ensure that it represents a more beneficial steel than that which is used today. Some steel grades are more prone than others to cause distortions, which must be compensated for during machining of industrial products. However, distortions can not only be linked to the alloying elements of steel but also to many other parameters, such as method of casting, distribution of alloying elements in the workpiece, how the workpieces are positioned in the heat furnace, the size of each part that needs to be heat treated, and the temperature and time of the heat treatment.

ACKNOWLEDGEMENTS

I am grateful for spending these 3 years of graduate studies. It has been a journey on which I met many intelligent and inspiring people whom helped me into the life of a researcher. For that reason, there are some people I wish to express my gratitude.

Thank you Andrey for being a great supervisor. I would like to express my sincerest gratitude for your help, the discussions we have had and the amount of time you have put into this. Thank you Thomas for giving me a great start and introduction to the world of metal cutting. I would never gone through with this if it was not for you. Thanks Pär for your always so open and welcoming attitude. You are always willing to help. I would like to acknowledge the effort from Staffan who made this possible in the first place.

All my previous colleagues at Swerea KIMAB, thanks for three great years and the many laughter's we shared together. Thank you Peter for introducing me into the world of gearbox manufacturing and for the good start within your group.

From the industrial partners, who have been involved in my work, I would like to thank Anna, Marianne, Rickard, Jan, Staffan, Patrik and Sara for guidance and a pleasant collaboration.

I would like to thank my family for your support. You are a bunch of fantastic persons and words cannot describe what you mean to me. And my dearest Matilda, you are so amazing! Thanks for all your support, love and encouragement.

Niclas Ånmark, Stockholm, 2016.

BIBLIOGRAPHY

1. Göransson M., Jönsson P.G. Ideas for process control of inclusion characteristics during steelmaking. *ISIJ Int.* 41 (2001) 42–46.
2. Hojo M., Nakao R., Umezaki T., Kawai H., Tanaka S., Fukumoto S. Oxide inclusion control in ladle and tundish for producing clean stainless steel. *ISIJ Int.* 36 (1996) 128–131.
3. Tanaka H., Nishihara R., Miura R., Tsujino R., Kimura T., Nishi T., Imoto T. Technology for cleaning of molten steel. *ISIJ Int.* 34 (1994) 868–875.
4. Zhul S.I., Guzenkov S.A., Sergeev V.I., Bod K.Y. Developing efficient charges for making ultra-clean steel. *Metallurgist* 47 (2003) 401–404.
5. Holappa L. On physico-chemical and technical limits in clean steel production. *Steel Res. Int.* 81 (2010) 869–874.
6. Zhang F.M. Study and design on clean steel production platform. *Appl. Mech. Mater.* 161 (2012) 37–41.
7. Deng Z., Zhu M. A new double calcium treatment method for clean steel refining. *Steel Res. Inst. Met.* 84 (2013) 519–525.
8. Mazumdar D. Tundish metallurgy: towards increased productivity and clean steel. *Trans. Indian Inst. Met.* 66 (2013) 597–610.
9. Ånmark N. *Inclusion characteristics and their link to tool wear in metal cutting of clean steels suitable for automotive applications.* (KTH Royal Institute of Technology, 2015).
10. Ånmark N., Björk T., Ganea A., Ölund P., Hogmark S., Karasev A., Jönsson P.G. The effect of inclusion composition on tool wear in hard part turning using PCBN cutting tools. *Wear* 334–335 (2015) 13–22.
11. Holappa L.E.K., Helle A.S. Inclusion control in high-performance steels. *J. Mater. Process. Technol.* 53 (1995) 177–186.

12. Väinölä R.V., Holappa L.E.K., Karvonen P.H.J. Modern steelmaking technology for special steels. *J. Mater. Process. Technol.* 53 (1995) 453–465.
13. Zhang L.F., Thomas B.G. State of the art in evaluation and control of steel cleanliness. *ISIJ Int.* 43 (2003) 271–291.
14. Suito I., Inoue R. Thermodynamics on control of inclusions composition in ultra-clean steels. *ISIJ Int.* 36 (1996) 528–536.
15. Tang Y. Effect of slag composition on inclusion control in LF-VD process for ultra-low oxygen alloyed structural steel. In *The 2nd international conference on mining engineering and metallurgical technology* (Elsevier, 2011).
16. Atkinson H.V., Shi G. Characterization of inclusions in clean steels: a review including the statistics of extremes methods. *Prog. Mater. Sci.* 48 (2003) 457–520.
17. Anderson C.W., Shi G., Atkinson H.V., Sellars C.M. The precision of methods using the statistics of extremes for the estimation of the maximum size of inclusions in clean steels. *Acta Mater.* 48 (2000) 4235–4246.
18. Anderson C.W., de Maré J., Rootzén H. Methods for estimating the sizes of large inclusions in clean steels. *Acta Mater.* 53 (2005) 2295–2304.
19. Ånmark N., Karasev A., Jönsson P.G. The effect of different non-metallic inclusions on the machinability of steels. *Materials.* 8 (2015) 751–783.
20. Faraji M., Wilcox D.P., Thackray R., Howe A.A., Todd I., Tsakirooulos P. Quantitative characterization of inclusions in continuously cast high-carbon steel. *Metall. Mater. Trans. B* 46 (2015) 2490–2502.
21. Bi Y., Karasev A., Jönsson P.G. Three-dimensional investigations of inclusions in ferroalloys. *Steel Res. Int.* 85 (2014) 659–669.
22. Janis D., Inoue R., Karasev A., Jönsson P.G. Application of different extraction methods for investigation of nonmetallic inclusions and clusters in steels and alloys. *Adv. Mater. Sci.*

- Eng.* 2014 (2014) 1–7.
23. Karasev A., Suito H. Analysis of size distributions of primary oxide inclusions in Fe-10 mass pct Ni-M (M=Si, Ti, Al, Zr, and Ce) alloy. *Metall. Mater. Trans. B* 30B (1999) 259–270.
 24. Wang X., Jiang Z. Deoxidation and inclusion control in stainless steel refining. *Adv. Mater. Res.* 968 (2014) 146–150.
 25. Wijk O., Brabie V. The purity of ferrosilicon and its influence on inclusion cleanliness of steel. *ISIJ Int.* 36 (1996) 132–135.
 26. Park J., Kang Y. Effect of ferrosilicon addition on the composition of inclusions in 16Cr-14Ni-Si Stainless Steel Melts. *Metall. Mater. Trans. B* 37 (2006) 791–797.
 27. Riyahimalayeri K., Ölund P., Selleby M. Oxygen activity calculations of molten steel: comparison with measured results. *Steel Res. Int.* 84 (2013) 136–145.
 28. Andersson L., Berggren K., Bodin J. *Steel and its heat treatment*. (Swerea IVF, 2012).
 29. Yamada M., Yan L., Takaku R., Ohsaki S., Miki K., Kajikawa K., Azuma T. Effects of alloying elements on the hardenability, toughness and the resistance of stress corrosion cracking in 1 to 3 mass % Cr low alloy steel. *ISIJ Int.* 54 (2014) 240–247.
 30. Ohtani S., Katayama S., Akasawa T., Bhattacharya D., Yaguchi H. Qualities of strand cast resulfurized free-machining steels. *J. Appl. Metalwork.* 4 (1986) 245–254.
 31. Yaguchi H. Effect of MnS inclusion size on machinability of low-carbon, leaded, resulfurized free-machining steel. *J. Appl. Metalwork.* 4 (1986) 214–225.
 32. Nordgren A., Melander A. Deformation behaviour of different types of inclusion during chip formation in turning of quenched and tempered steels. *Mater. Sci. Technol.* 5 (1989) 940–951.
 33. Nordgren A., Melander A. Tool wear and inclusion behaviour during turning of a calcium-treated quenched and tempered steel using coated cemented carbide tools. *Wear* 139 (1990) 209–223.

34. Nordgren A. *Tool wear and inclusion behaviour during machining of Ca-treated steels*. (KTH Royal Institute of Technology, 1993).
35. Gerth J.L. *Tribology at the Cutting Edge - a study of material transfer and damage mechanisms in metal cutting*. (Uppsala University, 2012).
36. Shaw M.C. *Metal cutting principles*. (Clarendon Press, 1984).
37. Ståhl J.E. *Metal cutting – theories and models*. (Lund University, 2012).
38. Tönshoff H.K., Stanske C. High productivity machining: materials and processes. In *Proceedings of the international conference on high productivity machining* (Elsevier, 1985).
39. Kiessling R. The influence of non-metallic inclusions on the properties of steel. *J. Met.* 21 (1969) 48–54.
40. Sadik I. *An introduction to cutting tools materials and applications*. (Elanders, 2013).
41. Huang Y., Chou Y.K., Liang S.Y. CBN tool wear in hard turning: a survey on research progresses. *Int. J. Adv. Manuf. Technol.* 35 (2007) 443–453.
42. Chou Y.K., Evans C.J. Cubic boron nitride tool wear in interrupted hard cutting. *Wear* 225-229 (1999) 234–245.
43. Barry J., Byrne G. Cutting tool wear in the machining of hardened steels part II: cubic boron nitride cutting tool wear. *Wear* 247 (2001) 152–160.
44. McKie A., Winzer J., Sigalas I., Herrmann M., Weiler L., Rödel J., Can N. Mechanical properties of cBN–Al composite materials. *Ceram. Int.* 37 (2011) 1-8.
45. Luo S.Y., Liao Y.S., Tsai Y.Y. Wear characteristics in turning high hardness alloy steel by ceramic and CBN tools. *J. Mater. Process. Technol.* 88 (1999) 114–121.
46. Davies M.A., Chou Y., Evans C.J. On chip morphology, tool wear and cutting mechanics in finish hard turning. *CIRP Ann.* 45 (1996) 77–82.
47. Poulachon G., Bandyopadhyay B., Jawahir I., Pheulpin S.,

- Seguin E. Wear behavior of CBN tools while turning various hardened steels. *Wear* 256 (2004) 302–310.
48. Nakayama K., Arai M., Kanda T. Machining characteristics of hard materials. *CIRP Ann.* 37 (1988) 89–92.
49. König W., Neises A. Wear mechanisms of ultrahard, non-metallic cutting materials. *Wear* 162-164 (1993) 12–21.
50. Farhat Z.N. Wear mechanism of CBN cutting tool during high-speed machining of mold steel. *Mater. Sci. Eng. A* 361 (2003) 100–110.
51. Trent E.M., Wright P.K. *Metal Cutting*. (Butterworth-Heinemann, 2000).
52. Zimmermann M., Lahres M., Viens D.V., Laube B.L. Investigations of the wear of cubic boron nitride cutting tools using Auger electron spectroscopy and X-ray analysis by EPMA. *Wear* 209 (1997) 241–246.
53. Chou Y.K., Evans C.J. Tool wear mechanism in continuous cutting of hardened tool steels. *Wear* 212 (1997) 59–65.
54. Chou Y.K., Evans C.J., Barash M.M. Experimental investigation on cubic boron nitride turning of hardened AISI 52100 steel. *J. Mater. Process. Technol.* 134 (2003) 1–9.
55. Ånmark N., Björk T. Steel characteristics and their link to tool wear in hard part turning of transmission components. *Wear* (2016).
56. Dos Santos A.L.B., Duarte M.A.V., Abrão A.M., Machado A.R. An optimisation procedure to determine the coefficients of the extended Taylor's equation in machining. *Int. J. Mach. Tools Manuf.* 39 (1999) 17–31.
57. Axinte D.A., Belluco W., De Chiffre L. Reliable tool life measurements in turning - an application to cutting fluid efficiency evaluation. *Int. J. Mach. Tools Manuf.* 41 (2001) 1003–1014.
58. Meng Q., Arsecularatne J.A., Mathew P. Calculation of optimum cutting conditions for turning operations using a machining theory. *Int. J. Mach. Tools Manuf.* 40 (2000)

- 1709-1733.
59. Bartarya G., Choudhury S.K. State of the art in hard turning. *Int. J. Mach. Tools Manuf.* 53 (2012) 1–14.
 60. Yaltese M.A., Chaoui K., Zeghib N., Boulanouar L., Rigal J.F. Hard machining of hardened bearing steel using cubic boron nitride tool. *J. Mater. Process. Technol.* 209 (2009) 1092–1104.
 61. Yao N., Wang Z.L. *Handbook of microscopy for nanotechnology*. (Kluwer academic publishers, 2005).
 62. Vander Voort G.F. *ASM Handbook, Metallography and Microstructures*. (ASM International, 2004).
 63. Wang Q. Measuring the wavelength of light wave with four-sides prism spectrograph. *Opt. Int. J. Light Electron Opt.* 124 (2013) 6874–6876.
 64. *SS-ISO 3685 Tool life testing with single-point turning tools*. (SIS, 1994).
 65. Borgh I. *Aspects of structural evolution in cemented carbide – carbide size, shape and stability*. (KTH Royal Institute of Technology, 2013).
 66. Goodhew P.J., Humphreys J., Beanland R. *Electron microscopy and analysis*. (Taylor and Francis, 2001).
 67. Bi Y., Karasev A.V., Jönsson P.G. Three dimensional evaluations of REM clusters in stainless steel. *ISIJ Int.* 54 (2014) 1266–1273.
 68. Bi Y. *Three dimensional determinations of inclusions in ferroalloys and steel samples*. (KTH Royal Institute of Technology, 2014).
 69. Rogante M. Wear characterisation and tool performance of sintered carbide inserts during automatic machining of AISI 1045 steel. *J. Mater. Process. Technol.* 209 (2009) 4776–4783.
 70. Sundararajan G., Roy M. Hardness testing. *Encycl. Mater. Sci. Technol.* 3728–3736 (1999).
 71. Raj B., Bhanu Sankara Rao K. Mechanical testing. *Encycl. Mater. Sci. Technol.* 5277–5291 (2001).

72. Biwa S., Storåkers B. An analysis of fully plastic Brinell indentation. *J. Mech. Phys. Solids* 43 (1995) 1303–1333.
73. Lou D., Cui K., Jia Y. Study on the machinability of resulfurized composite free-cutting steels. *J. Mater. Eng. Perform.* 6 (1997) 215–218.
74. Ramanujachar K., Subramanian S.V. Micromechanisms of tool wear in machining free cutting steels. *Wear* 197 (1996) 45–55.
75. Liu H., Chen W. Effect of total oxygen content on the machinability of low carbon resulfurized free cutting steel. *Steel Res. Int.* 83 (2012) 1172–1179.
76. Fang X.D., Zhang D. An investigation of adhering layer formation during tool wear progression in turning of free-cutting stainless steel. *Wear* 197 (1996) 169–178.
77. Ray K.K., Das J., Dixit A., Chakraborty M., Chakravorty S., Guha S.N. Effect of cold deformation on the machinability of a free cutting steel. *Mater. Manuf. Process.* 21 (2006) 333–340.
78. Kiessling R. *Non-metallic inclusions in steel - part 5.* (The Institute of Metals, 1989).
79. Leung C.H., Vlack L.H. Solubility limits in binary (Ca,Mn) chalcogenides. *J. Am. Ceram. Soc.* 62 (1979) 613–616.
80. Bletton O., Duet R., Pedarre P. Influence of oxide nature on the machinability of 316L stainless steels. *Wear* 139 (1990) 179-193.
81. Harcsik B., Karoly G. Controlling nozzle clogging by secondary steelmaking without reheating. *Steel Res. Int.* 84 (2013) 129-135.
82. Väinölä R., Karvonen P., Helle L.W. Establishment of calcium treatment practices at Ovako - historical development and evaluation of alternative methods. In *Scaninject 4 - proceedings of the 4th international conference on injection metallurgy.* (MEFOS, 1986).
83. Ånmark N., Björk T., Karasev A., Jönsson P.G. Effect of different inclusions on mechanical properties and machinability of 20NiCrMo carburizing steels. In *the 6th*

- international congress on the science and technology of steelmaking*. (China Machine Press, 2015).
84. Toppo V., Singh S.B., Ray K.K. Wear resistance of annealed plain carbon steels in pre-strained condition. *Wear* 266 (2009) 907–916.
 85. Abouei V., Saghafian H., Kheirandish S. Effect of microstructure on the oxidative wear behavior of plain carbon steel. *Wear* 262 (2007) 1225–1231.
 86. Zhang M., Kelly P.M. The morphology and formation mechanism of pearlite in steels. *Mater. Charact.* 60 (2009) 545–554.
 87. Van Bohemen S.M.C., Sietsma J. The kinetics of bainite and martensite formation in steels during cooling. *Mater. Sci. Eng. A* 527 (2010) 6672–6676.
 88. Jawahir I.S. The chip control factor in machinability assessments: recent trends. *J. Mech. Work. Technol.* 17 (1988) 213–224.
 89. Jawahir I.S. The tool restricted contact effect as a major influencing factor in chip breaking: an experimental analysis. *CIRP Ann.* 37 (1988) 121–126.
 90. Ånmark N., Lövquist S., Vosough M., Björk T. The effect of cleanliness and micro hardness on the machinability of carburizing steel grades suitable for automotive applications. *Steel Res. Int.* 87 (2016) 403–412.
 91. Hall E.O. The deformation and ageing of mild steel: III discussion of results. *Proc. Phys. Soc. Sect. B* 64 (1951) 747–753.
 92. Petch N.J. The influence of some substitutional alloys on the cleavage of ferritic steels. *Acta Metall.* 35 (1987) 2027–2034.
 93. Seok M.Y., Choi I.C., Moon J., Kim S., Ramamurty U., Jang J.I. Estimation of the Hall-Petch strengthening coefficient of steels through nanoindentation. *Scr. Mater.* 87 (2014) 49–52.
 94. Ånmark N., Karasev A., Jönsson P.G. The influence of microstructure and non-metallic inclusions on the

- machinability of clean steels. *Steel Res. Int.* (2016).
95. Jiang L., Cui K., Hänninen H. Effects of the composition, shape factor and area fraction of sulfide inclusions on the machinability of re-sulfurized of free machining steel. *J. Mater. Process. Technol.* 58 (1996) 160-165.
 96. Larsson A., Rупpi S. Structure and composition of built-up layers on coated tools during turning of Ca-treated steel. *Mater. Sci. Eng. A* 313 (2001) 160-169.
 97. Leung C.H., Van Vlack L.H. Solution and precipitation hardening in (Ca, Mn) sulfides and selenides. *Metall. Trans. A* 12 (1981) 987-991.
 98. Brion J.M., Sander B., Pierson G., Lepage J., Von Stebut J. Mechanisms of built-up layer formation on turning tools: Influence of tool and workpiece. *Wear* 154 (1992) 225-239.
 99. Angseryd J., Olsson E., Andrén H.O. Effect of workpiece sulphur content on the degradation of a PCBN tool material. *Int. J. Refract. Met. Hard Mater.* 29 (2011) 674-680.
 100. Väinölä R., Heiskala M., Huhtiranta M. Bloom casting improves the properties of better machinable Imatra M steels. In *scaninject VI, 6th international conference on refining processes.* (MEFOS, 1992).
 101. Ueda T., Al Huda M., Yamada K., Nakayama K. Temperature measurement of CBN tool in turning of high hardness steel. *Ann. CIRP* 48 (1999) 63-66.
 102. Harju E., Kivivuori S., Korhonen A.S. Formation of a wear resistant non-metallic protective layer on PVD-coated cutting and forming tools. *Surf. Coatings Technol.* 112 (1999) 98-102.